

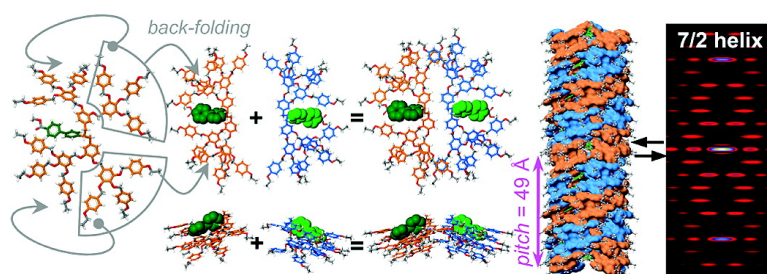
Article

## Expanding the Structural Diversity of Self-Assembling Dendrons and Supramolecular Dendrimers via Complex Building Blocks

Virgil Percec, Betty C. Won, Mihai Peterca, and Paul A. Heiney

*J. Am. Chem. Soc.*, **2007**, 129 (36), 11265-11278 • DOI: 10.1021/ja073714j • Publication Date (Web): 17 August 2007

Downloaded from <http://pubs.acs.org> on February 14, 2009



### More About This Article

Additional resources and features associated with this article are available within the HTML version:

- Supporting Information
- Links to the 11 articles that cite this article, as of the time of this article download
- Access to high resolution figures
- Links to articles and content related to this article
- Copyright permission to reproduce figures and/or text from this article

[View the Full Text HTML](#)

## Expanding the Structural Diversity of Self-Assembling Dendrons and Supramolecular Dendrimers via Complex Building Blocks

Virgil Percec,<sup>\*,†</sup> Betty C. Won,<sup>†</sup> Mihai Peterca,<sup>†,‡</sup> and Paul A. Heiney<sup>‡</sup>

Contribution from the Roy & Diana Vagelos Laboratories, Department of Chemistry, University of Pennsylvania, Philadelphia, Pennsylvania 19104-6323, and Department of Physics and Astronomy, University of Pennsylvania, Philadelphia, Pennsylvania 19104-6396

Received May 23, 2007; Revised Manuscript Received July 13, 2007; E-mail: percec@sas.upenn.edu

**Abstract:** The design and synthesis of the first examples of AB<sub>4</sub> and AB<sub>5</sub> dendritic building blocks with complex architecture are reported. Structural and retrostructural analysis of supramolecular dendrimers self-assembled from hybrid dendrons based on different combinations of AB<sub>4</sub> and AB<sub>5</sub> building blocks with AB<sub>2</sub> and AB<sub>3</sub> benzyl ether dendrons demonstrated that none of these new hybrid dendrons exhibit the previously encountered conformations of libraries of benzyl ether dendrons. These hybrid dendrons enabled the discovery of some highly unusual tapered and conical dendrons generated by the intramolecular back-folding of their repeat units and of their apex. The new back-folded tapered dendrons have double thickness and self-assemble into pine-tree-like columns exhibiting a long-range 7/2 helical order. The back-folded conical dendrons self-assemble into spherical dendrimers. Non-back-folded truncated conical dendrons were also discovered. They self-assemble into spherical dendrimers with a less densely packed center. The discovery of dendrons displaying a novel crown-like conformation is also reported. Crown-like dendrons self-assemble into long-range 5/1 helical pyramidal columns. The long-range 7/2 and 5/1 helical structures were established by applying, for the first time, the helical diffraction theory to the analysis of X-ray patterns obtained from oriented fibers of supramolecular dendrimers.

Dendrimers and dendrons<sup>1</sup> synthesized by divergent<sup>2</sup> and convergent methods<sup>3</sup> are extensively explored at the interface between chemistry, biology, physics, medicine, and nanoscience.<sup>4</sup> Self-assembling dendrons<sup>5–11</sup> provide some of the most influential complex architectures of nonbiological origins that are currently used in our laboratory to investigate the transfer of molecular information from the primary structure to the three-dimensional structure.<sup>9,10</sup> The hierarchical processing of complex structural information at multiple-length scales<sup>9,10</sup> is responsible for the creation of order and functions<sup>12</sup> and, therefore, represents one of the most fundamental principles of chemistry.

Our laboratory is involved in the elaboration of amphiphilic self-assembling dendrons, including hybrid dendrons based on various combinations of AB and constitutional isomeric AB<sub>2</sub> and AB<sub>3</sub> repeat units. This self-assembly process is monitored by retrostructural analysis. This methodology facilitates the elucidation of the mechanism by which the primary structure is transferred on multiple-length scales during the generation

of order and function in 2-D and 3-D periodic and quasiperiodic supramolecular systems. This publication reports the design of the first examples of complex AB<sub>4</sub> and AB<sub>5</sub> dendritic building blocks and demonstrates their capability to expand the structural diversity and complexity of self-assembling dendrons and of their supramolecular dendrimers.

### Results and Discussion

**Synthesis of the AB<sub>4</sub> Building Block 13.** The strategy involved in the synthesis of the AB<sub>4</sub> and AB<sub>5</sub> building blocks was inspired from a methodology delineated for the synthesis

<sup>†</sup> Department of Chemistry, University of Pennsylvania.

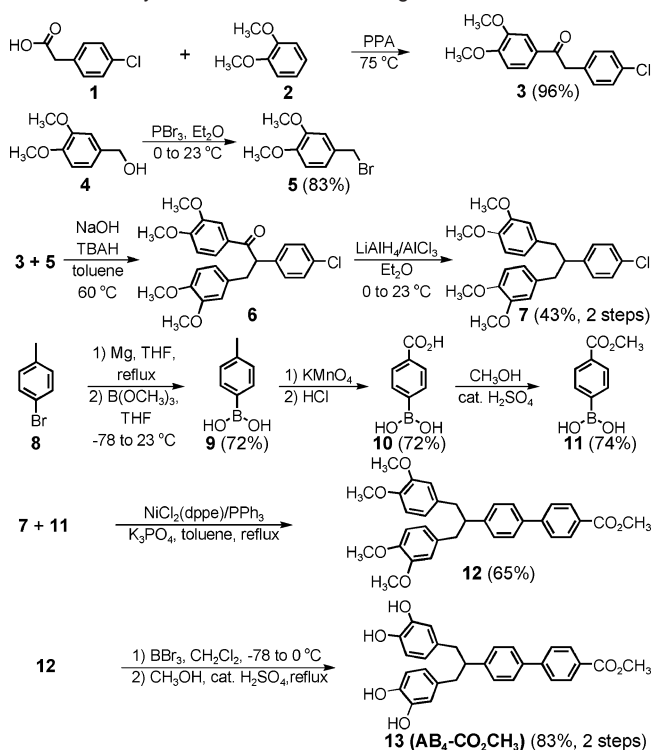
<sup>‡</sup> Department of Physics and Astronomy, University of Pennsylvania.

- (1) (a) Fréchet, J. M. J.; Tomalia, D. A., Eds. *Dendrimers and Other Dendritic Polymers*; Wiley: New York 2001. (b) Newkome, G. R.; Moorefield, C. N.; Vögtle, F. *Dendrimers and Dendrons*; Wiley-VCH: Weinheim, 2001. (c) Buhleier, E.; Wehner, W.; Vögtle, F. *Synthesis* **1978**, 155–158. (d) Tomalia, D. A.; Baker, H.; Dewald, J.; Hall, M.; Kallos, G.; Martin, S.; Roeck, J.; Ryder, J.; Smith, P. *Polym. J.* **1985**, *17*, 117–132. (e) Newkome, G. R.; Yao, Z.; Baker, G. R.; Gupta, V. K. *J. Org. Chem.* **1985**, *50*, 2003–2004. (f) Hawker, C. J.; Fréchet, J. M. J. *J. Am. Chem. Soc.* **1990**, *112*, 7638–7647. (g) Miller, T. M.; Neenan, T. X. *Chem. Mater.* **1990**, *2*, 346–349.

- (4) (a) Moore, J. S. *Acc. Chem. Res.* **1997**, *30*, 402–413. (b) Kim, Y.; Zimmerman, S. C. *Curr. Opin. Chem. Biol.* **1998**, *2*, 733–742. (c) Seebach, D.; Rheiner, P. B.; Greiveldinger, G.; Butz, T.; Sellner, H. *Top. Curr. Chem.* **1998**, *197*, 125–164. (d) Majoral, J.-P.; Caminade, A.-M. *Top. Curr. Chem.* **1998**, *197*, 79–124. (e) Smith, D. K.; Diederich, F. *Chem.-Eur. J.* **1998**, *4*, 1353–1361. (f) Fischer, M.; Vögtle, F. *Angew. Chem., Int. Ed.* **1999**, *38*, 885–905. (g) Bosman, A. W.; Janssen, H. M.; Meijer, E. W. *Chem. Rev.* **1999**, *99*, 1665–1688. (h) Astruc, D.; Chardac, F. *Chem. Rev.* **2001**, *101*, 2991–3024. (i) Haag, R. *Chem.-Eur. J.* **2001**, *7*, 327–335. (j) Hecht, S.; Fréchet, J. M. J. *Angew. Chem., Int. Ed.* **2001**, *40*, 74–91. (k) Tully, D. C.; Fréchet, J. M. J. *Chem. Commun.* **2001**, 1229–1239. (l) Stiriba, S.-E.; Frey, H.; Haag, R. *Angew. Chem., Int. Ed.* **2002**, *41*, 1329–1334. (m) Esfand, R.; Tomalia, D. A. *Drug Discovery Today* **2001**, *6*, 427–436. (n) Gillies, E. R.; Fréchet, J. M. J. *Drug Discovery Today* **2005**, *10*, 35–43. (o) Jiang, D.-L.; Aida, T. *Prog. Polym. Sci.* **2005**, *30*, 403–422. (p) Van de Coevering, R.; Gebbink, R. J. M. K.; Van Koten, G. *Prog. Polym. Sci.* **2005**, *30*, 474–490. (q) Caminade, A.-M.; Majoral, J.-P. *Prog. Polym. Sci.* **2005**, *30*, 491–505. (r) Boas, U.; Heegaard, P. M. H. *Chem. Soc. Rev.* **2004**, *33*, 43–63. (s) Grinstaff, M. W. *Chem.-Eur. J.* **2002**, *8*, 2838–2846. (t) Grayson, S. M.; Fréchet, J. M. J.; *Chem. Rev.* **2001**, *101*, 3819–3867. (u) Shabat, D. *J. Polym. Sci., Part A: Polym. Chem.* **2006**, *44*, 1569–1578. (v) Frauenrath, H. *Prog. Polym. Sci.* **2005**, *30*, 325–384.

of conformationally flexible AB<sub>2</sub> building blocks.<sup>13</sup> The synthesis of the AB<sub>4</sub> building block **13** is outlined in Scheme 1. The first step involves the acylation of 4-chlorophenylacetic acid (**1**) with veratrole (**2**) in freshly prepared polyphosphoric acid<sup>14</sup> at 75 °C to yield ketone **3** in 96% yield. This procedure was previously employed in our laboratory<sup>13</sup> since it replaces the need to form the acid chloride required for Friedel–Crafts acylations. Bromination of 3,4-dimethoxybenzyl alcohol (**4**) with PBr<sub>3</sub> in Et<sub>2</sub>O<sup>15</sup> generated bromide **5** in 83% yield. The enolate alkylation of **3** with 3,4-dimethoxybenzyl bromide (**5**) under phase-transfer conditions<sup>13</sup> gave ketone **6**, which was reduced

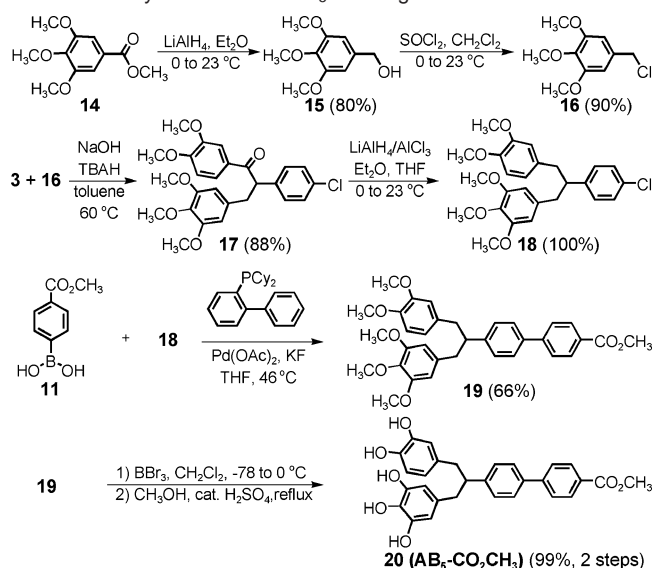
**Scheme 1.** Synthesis of the AB<sub>4</sub> Building Block



- (5) For selected recent reviews on supramolecular dendrimers self-organized into periodic arrays, see: (a) Zimmerman, S. C. *Curr. Opin. Colloid Interface Sci.* **1997**, *2*, 89–99. (b) Matthews, O. A.; Shipway, A. N.; Stoddart, J. F. *Prog. Polym. Sci.* **1998**, *23*, 1–56. (c) Fischer, M.; Vögtle, F. *Angew. Chem., Int. Ed.* **1999**, *38*, 885–905. (d) Emrick, T.; Fréchet, J. M. J. *Curr. Opin. Colloid Interface Sci.* **1999**, *4*, 15–23. (e) Schlenk, C.; Frey, H. *Monatsh. Chem.* **1999**, *130*, 3–14. (f) Smith, D. K.; Diederich, F. *Top. Curr. Chem.* **2000**, *210*, 183–227. (g) Ponomarenko, S. A.; Boiko, N. I.; Shibaev, V. P. *Polym. Sci. Ser. C* **2001**, *43*, 1–45. (h) Guillon, D.; Deschenaux, R. *Curr. Opin. Solid State Mater. Sci.* **2002**, *6*, 515–525. (i) Tschierske, C. *Curr. Opin. Colloid Interface Sci.* **2002**, *7*, 69–80. (j) Diele, S. *Curr. Opin. Colloid Interface Sci.* **2002**, *7*, 333–342. (k) Caminade, A.-M.; Turrin, C.-O.; Sutra, P.; Majoral, J.-P. *Curr. Opin. Colloid Interface Sci.* **2003**, *8*, 282–295. (l) Smith, D. K.; Hirst, A. R.; Love, C. S.; Hardy, J. G.; Brignell, S. V.; Huang, B. *Prog. Polym. Sci.* **2005**, *30*, 220–293. (m) Percec, V. *Philos. Trans. R. Soc. London, Ser. A* **2006**, *364*, 2709–2719. (n) Rudick, J. C.; Percec, V. *New J. Chem.* **2007**, *31*, 1083–1096. (o) Donnio, B.; Guillon, D. *Adv. Polym. Sci.* **2006**, *201*, 45–155.
- (6) For selected examples of amphiphilic self-assembling dendrons and self-organizing dendrimers based on AB<sub>3</sub> repeat units, see: (a) Percec, V.; Johansson, G.; Heck, J.; Ungar, G.; Batty, S. V. *J. Chem. Soc., Perkin Trans. 1* **1993**, 1411–1420. (b) Johansson, G.; Percec, V.; Ungar, G.; Abramic, D. *J. Chem. Soc., Perkin Trans. 1* **1994**, 447–459. (c) Percec, V.; Johansson, G.; Ungar, G.; Zhou, J. *J. Am. Chem. Soc.* **1996**, *118*, 9855–9866. (d) Balagurusamy, V. S. K.; Ungar, G.; Percec, V.; Johansson, G. *J. Am. Chem. Soc.* **1997**, *119*, 1539–1555. (e) Hudson, S. D.; Jung, H.-T.; Percec, V.; Cho, W.-D.; Johansson, G.; Ungar, G.; Balagurusamy, V. S. K. *Science* **1997**, *278*, 449–452. (f) Percec, V.; Cho, W.-D.; Mosier, P. E.; Ungar, G.; Yearley, D. J. *J. Am. Chem. Soc.* **1998**, *120*, 11061–11070. (g) Ungar, G.; Percec, V.; Holerca, M. N.; Johansson, G.; Heck, J. *A. Chem.—Eur. J.* **2000**, *6*, 1258–1266. (h) Percec, V.; Cho, W.-D.; Möller, M.; Prokhorova, S. A.; Ungar, G.; Yearley, D. J. *J. Am. Chem. Soc.* **2000**, *122*, 4249–4250. (i) Percec, V.; Cho, W.-D.; Ungar, G. *J. Am. Chem. Soc.* **2000**, *122*, 10273–10281. (j) Dukeson, D. R.; Ungar, G.; Balagurusamy, V. S. K.; Percec, V.; Johansson, G. A.; Glodde, M. *J. Am. Chem. Soc.* **2003**, *125*, 15974–15980. (k) Percec, V.; Glodde, M.; Johansson, G.; Balagurusamy, V. S. K.; Heiney, P. A. *Angew. Chem., Int. Ed.* **2003**, *42*, 4338–4342. (l) Malthête, J. *New J. Chem.* **1996**, *20*, 925–928. (m) Percec, V.; Peterca, M.; Sienkowska, M. J.; Iliés, M. A.; Aqad, E.; Smidrkal, J.; Heiney, P. A. *J. Am. Chem. Soc.* **2006**, *128*, 3324–3334. (n) Percec, V.; Holerca, M. N.; Nummelin, S.; Morrison, J. L.; Glodde, M.; Smidrkal, J.; Peterca, M.; Rosen, B. M.; Uchida, S.; Balagurusamy, V. S. K.; Sienkowska, M. J.; Heiney, P. A. *Chem.—Eur. J.* **2006**, *12*, 6216–6241.
- (7) For selected examples of amphiphilic self-assembling dendrons based on AB<sub>2</sub> repeat units, see: (a) Percec, V.; Cho, W.-D.; Ungar, G.; Yearley, D. J. *P. Angew. Chem., Int. Ed.* **2000**, *39*, 1598–1602. (b) Percec, V.; Cho, W.-D.; Ungar, G.; Yearley, D. J. *J. Am. Chem. Soc.* **2001**, *123*, 1302–1315. (c) Suárez, M.; Lehn, J.-M.; Zimmerman, S. C.; Skoulios, A.; Heinrich, B. *J. Am. Chem. Soc.* **1998**, *120*, 9526–9532.
- (8) For examples of amphiphilic self-assembling dendrons based on combinations of AB, AB<sub>2</sub>, and AB<sub>3</sub> benzyl ether and other hybrid dendrons, see: (a) Percec, V.; Mitchell, C. M.; Cho, W.-D.; Uchida, S.; Glodde, M.; Ungar, G.; Zeng, X.; Liu, Y.; Balagurusamy, V. S. K.; Heiney, P. A. *J. Am. Chem. Soc.* **2004**, *126*, 6078–6094. (b) Percec, V.; Smidrkal, J.; Peterca, M.; Mitchell, C. M.; Nummelin, S.; Dulcey, A. E.; Sienkowska, M. J.; Heiney, P. A. *Chem.—Eur. J.* **2007**, *13*, 3989–4007.
- (9) For examples of dendrons that self-assemble and co-assemble into supramolecular lattices and/or complex supramolecules, see: (a) Percec, V.; Ahn, C.-H.; Bera, T. K.; Ungar, G.; Yearley, D. J. *Chem.—Eur. J.* **1999**, *5*, 1070–1083. (b) Percec, V.; Bera, T. K.; Glodde, M.; Fu, Q.; Balagurusamy, V. S. K.; Heiney, P. A. *Chem.—Eur. J.* **2003**, *9*, 921–935. (c) Percec, V.; Imam, M. R.; Bera, T. K.; Balagurusamy, V. S. K.; Peterca, M.; Heiney, P. A. *Angew. Chem., Int. Ed.* **2005**, *44*, 4739–4745.
- (10) For new periodic and quasi-periodic lattices self-organized from supramolecular dendrimers, see: (a) Ungar, G.; Liu, Y.; Zeng, X.; Percec, V.; Cho, W.-D. *Science* **2003**, *299*, 1208–1211. (b) Zeng, X.; Ungar, G.; Liu, Y.; Percec, V.; Dulcey, A. E.; Hobbs, J. K. *Nature* **2004**, *428*, 157–160. (c) Chvalun, S. N.; Shcherbina, M. A.; Yakunin, A. N.; Blackwell, J.; Percec, V. *Polym. Sci. Ser. A* **2007**, *49*, 158–167.
- (11) For additional examples of self-assembling amphiphilic dendrons, see: (a) Kim, C.; Kim, K. T.; Chang, Y.; Song, H. H.; Cho, T.-Y.; Jeon, H.-J. *J. Am. Chem. Soc.* **2001**, *123*, 5586–5587. (b) Cho, B.-K.; Jain, A.; Gruner, S. M.; Wiesner, U. *Science* **2004**, *305*, 1598–1601. (c) Cho, B.-K.; Jain, A.; Mahajan, S.; Ow, H.; Gruner, S. M.; Wiesner, U. *J. Am. Chem. Soc.* **2004**, *126*, 4070–4071.

directly to the methylene group by using a LiAlH<sub>4</sub>/AlCl<sub>3</sub>·Et<sub>2</sub>O complex.<sup>13,16</sup> The aryl chloride **7** was obtained in 43% yield. The boronic reagent of bromotoluene (**8**), followed by addition of trimethylborate to generate tolylboronic acid (**9**)<sup>17</sup> in 72% yield. Benzylic oxidation of **9** with KMnO<sub>4</sub> in aqueous NaOH yielded, after acidification, the carboxylic acid **10**,<sup>18</sup> which was esterified under acidic conditions with methanol to give **11**<sup>19</sup> in 74% yield. Nickel-catalyzed Suzuki coupling<sup>20</sup> of aryl chloride **7** and

- (12) For examples of functions mediated via the 3-D structures generated by self-assembling dendrons, see: (a) Percec, V.; Heck, J.; Tomazos, D.; Falkenberg, F.; Blackwell, H.; Ungar, G. *J. Chem. Soc., Perkin Trans. 1* **1993**, 2799–2811. (b) Percec, V.; Heck, J. A.; Tomazos, D.; Ungar, G. *J. Chem. Soc., Perkin Trans. 2* **1993**, 2381–2388. (c) Percec, V.; Tomazos, D.; Heck, J.; Blackwell, H.; Ungar, G. *J. Chem. Soc., Perkin Trans. 2* **1994**, 31–44. (d) Percec, V.; Ahn, C.-H.; Barboiu, B. *J. Am. Chem. Soc.* **1997**, *119*, 12978–12979. (e) Percec, V.; Ahn, C.-H.; Ungar, G.; Yearley, D. J. P.; Möller, M.; Sheiko, S. S. *Nature* **1998**, *391*, 161–164. (f) Percec, V.; Glodde, M.; Bera, T. K.; Miura, Y.; Shiyankovskaya, I.; Singer, K. D.; Balagurusamy, V. S. K.; Heiney, P. A.; Schnell, I.; Rapp, A.; Spiess, H.-W.; Hudson, S. D.; Duan, H. *Nature* **2002**, *419*, 384–387. (g) Percec, V.; Dulcey, A. E.; Balagurusamy, V. S. K.; Miura, Y.; Smidrkal, J.; Peterca, M.; Nummelin, S.; Edlund, U.; Hudson, S. D.; Heiney, P. A.; Duan, H.; Magonov, S. N.; Vinogradov, S. A. *Nature* **2004**, *430*, 764–768. (h) Percec, V.; Rudick, J. G.; Peterca, M.; Wagner, M.; Obata, M.; Mitchell, C. M.; Cho, W.-D.; Balagurusamy, V. S. K.; Heiney, P. A. *J. Am. Chem. Soc.* **2005**, *127*, 15257–15264.
- (13) (a) Percec, V.; Kawasumi, M. *Macromolecules* **1991**, *24*, 6318–6324. (b) Percec, V.; Kawasumi, M. *Macromolecules* **1992**, *25*, 3843–3850. (c) Percec, V.; Chu, P. W.; Kawasumi, M. *Macromolecules* **1994**, *27*, 4441–4453. (d) Percec, V.; Chu, P.; Ungar, G.; Zhou, J. *J. Am. Chem. Soc.* **1995**, *117*, 11441–11454.
- (14) (a) Napolitano, E.; Giannone, E.; Fiaschi, R.; Marsili, A. *J. Org. Chem.* **1983**, *48*, 3653–3657. (b) Alessio, E. N.; Tombari, D. G.; Iglesias, G. Y. M.; Aguirre, J. M. *Can. J. Chem.* **1987**, *65*, 2568–2574.
- (15) Zumbunn, A. *Synthesis* **1998**, *9*, 1357–1361.
- (16) (a) Nystrom, R. F.; Berger, C. R. *J. Am. Chem. Soc.* **1958**, *80*, 2896–2898. (b) Albrecht, W. L.; Gustafson, D. H.; Horgan, S. W. *J. Org. Chem.* **1972**, *37*, 3355–3357.
- (17) (a) Seeman, W.; Johnson, J. R. *J. Am. Chem. Soc.* **1931**, *53*, 711–723. (b) Chan, K. S.; Zhou, X. A.; Au, M. T.; Tam, C. Y. *Tetrahedron* **1995**, *51*, 3129–3136.
- (18) (a) Michaelis, A.; Richter, E. *Justus Liebigs Ann. Chem.* **1901**, *315*, 26–40. (b) Matsubara, H.; Seto, K. J.; Tahara, T.; Takahashi, S. *Bull. Chem. Soc. Jpn.* **1989**, *62*, 3896–3901.
- (19) Tong, A. J.; Yamauchi, A.; Hayashita, T.; Zhang, Z. Y.; Smith, B. D.; Teramae, N. *Anal. Chem.* **2001**, *73*, 1530–1536.

**Scheme 2.** Synthesis of the AB<sub>5</sub> Building Block

4-methoxycarbonylphenylboronic acid (**11**) provided **12**, which was demethylated with  $\text{BBr}_3$ <sup>13,21</sup> in  $\text{CH}_2\text{Cl}_2$ . During this step, part of the ester of **12** was cleaved. Re-esterification provided the desired AB<sub>4</sub> **13** in 83% yield.

**Synthesis of the AB<sub>5</sub> Building Block 20.** The AB<sub>5</sub> building block **20** was synthesized in a fashion analogous to the synthesis of **13** (Scheme 2). The first step involves the reduction of methyl 3,4,5-trimethoxybenzoate with  $\text{LiAlH}_4$  to 3,4,5-trimethoxybenzyl alcohol (**15**)<sup>22</sup> (80% yield). Chlorination of **15** with  $\text{SOCl}_2$  generated **16**<sup>23</sup> in 90% yield. The enolate alkylation of **3** with the chloride **16** under phase-transfer conditions<sup>13</sup> gave ketone **17** in 88% yield. Reduction of ketone **17** with a  $\text{LiAlH}_4/\text{AlCl}_3 \cdot \text{Et}_2\text{O}$  complex<sup>13,16</sup> gave aryl chloride **18** in quantitative yield. Pd(0)-catalyzed Suzuki coupling of **18** with **11** by using 2-(dicyclohexylphosphino)biphenyl<sup>24</sup> as catalyst provided ester **19**. Demethylation of **19** with  $\text{BBr}_3$ <sup>13,21</sup> in  $\text{CH}_2\text{Cl}_2$ , followed by re-esterification, produced the AB<sub>5</sub> building block **20** in 99% yield.

**Synthesis of the Library of Self-Assembling AB<sub>4</sub> Hybrid Dendrons.** Synthesis of self-assembling AB<sub>4</sub> dendrons involves an iterative synthetic procedure<sup>6d,f,h,i,7b,25</sup> previously developed by our group to synthesize the benzyl halides **22–29** (Scheme 3). This method consists of the  $\text{LiAlH}_4$  reduction of an ester to a benzyl alcohol, followed by chlorination with  $\text{SOCl}_2$  in the presence of the proton trap 2,6-di-*tert*-butyl-4-methylpyridine,<sup>6d</sup> and then alkylation of a hydroxybenzoate. Tetraalkylation of building block **13** with halides **21–29** using  $\text{K}_2\text{CO}_3$ <sup>25</sup> in DMF produced the new self-assembling benzyl ether dendrons **30–38** in 15–77% yield (Scheme 3). Reduction of **30, 31, 34, 36,** and **38** with  $\text{LiAlH}_4$  yielded **39–43**, respectively, in 61–86% yield, while saponification of dendron **36** generated acid **44** in

64% yield. Acetylation of **42** using acetic anhydride and pyridine formed the acetate **45** in 58% yield. The purity of all self-assembling dendrons was 99+% (HPLC).

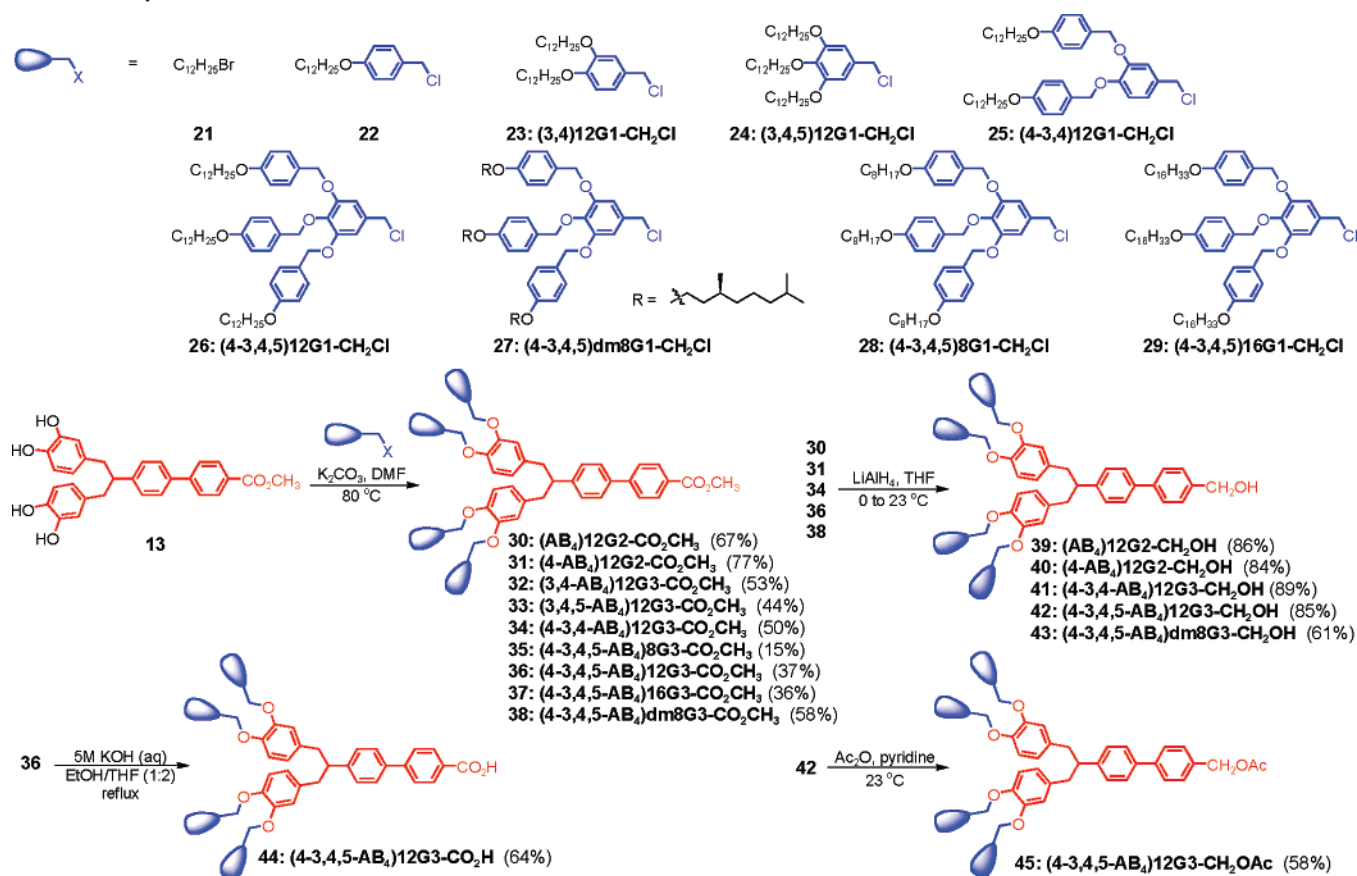
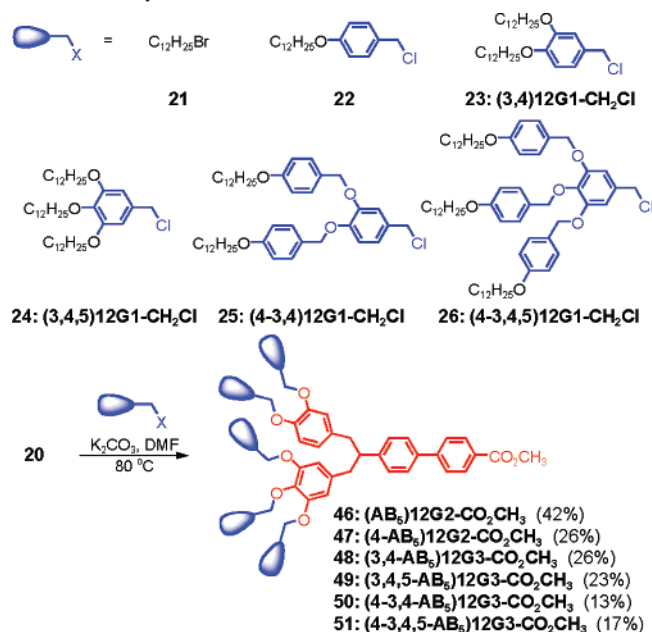
**Synthesis of the Library of Self-Assembling AB<sub>5</sub> Hybrid Dendrons.** Scheme 4 illustrates the synthesis of self-assembling AB<sub>5</sub> dendrons via a route analogous to that used in the synthesis of self-assembling AB<sub>4</sub> dendrons. Pentaalkylation of the AB<sub>5</sub> building block **20** with halides **21–26** using  $\text{K}_2\text{CO}_3$ <sup>25</sup> in DMF produced the new self-assembling dendrons **46–51** in 17–42% yields. The purity of the AB<sub>5</sub> dendrons was 99+% (HPLC).

**Strategy Employed in the Structural and Retrostructural Analysis of the Library of Supramolecular Dendrimers.** The structural and retrostructural analysis of all supramolecular dendrimers was performed by a methodology elaborated in our laboratory.<sup>6c,d,m,7b,8–10,12</sup> This involves a combination of analytical methods that includes <sup>1</sup>H and <sup>13</sup>C NMR, MALDI-TOF, high-performance liquid chromatography (HPLC), differential scanning calorimetry (DSC), thermal optical polarized microscopy (TOPM), experimental density ( $\rho_{20}$ ), and small- and wide-angle X-ray diffraction (XRD) experiments performed as a function of temperature on powder and oriented fibers, and reconstruction of the XRD data and electron density maps, together with molecular modeling. Details of the structural and retrostructural analysis, performed as elaborated and reported previously,<sup>6c,d,m,7b,8–10,12</sup> are presented in Supporting Tables ST1–ST4. The retrostructural analysis strategy outlined in Scheme 5 gives information on the transfer of structural information from the primary structure of the dendrons to their secondary, tertiary, and quaternary structures. The new dendron conformations and supramolecular dendrimer architectures and lattices discovered during this investigation are marked in Scheme 5 with dotted rectangles. These structures will be discussed in more detail. The DSC traces of both libraries are in Supporting Figures SF1–SF3. Thermal transitions, their enthalpy changes, and the phase assignments by XRD experiments for the AB<sub>4</sub>-based supramolecular dendrimers are summarized in Table 1. The measured d-spacings and the retrostructural analysis of the corresponding lattices assembled from the AB<sub>4</sub> library are reported in ST1 and ST2. The thermal transitions, d-spacings, and the retrostructural analysis of the AB<sub>5</sub> library are reported in Table 2, ST3, and ST4. During the structural and retrostructural analysis, the short names used for the dendrons follow the nomenclature used in previous publications from our laboratory.<sup>6m,7b,8a</sup> This nomenclature permits a straightforward visualization of the dendritic architecture in the absence of a reaction scheme.

**Structural and Retrostructural Analysis of the AB<sub>4</sub> Library.** The AB<sub>4</sub> (Scheme 1) and AB<sub>5</sub> (Scheme 2) building blocks are first-generation dendrons containing a tetrahedral branching point, four or five phenol groups, and an ester group. Therefore, the alkylation of these dendrons provides second-generation dendrons even when the electrophile is an *n*-alkyl halide (Schemes 3 and 4). The second branching points incorporated in the AB<sub>4</sub> and AB<sub>5</sub> dendron are based on aromatic–aliphatic ether or aromatic benzyl ether repeat units. This combination of branching points with highly dissimilar conformational freedom has not been employed in previous examples of self-assembling hybrid dendrons.<sup>8b</sup>

The main structural events of the retrostructural analysis results shown in SF1–SF3 are summarized in Scheme 6. (AB<sub>4</sub>)-12G2-CO<sub>2</sub>CH<sub>3</sub> (**30**) adopts a half-disc conformation that self-

- (20) (a) Percec, V.; Bae, J.-Y.; Zhao, M.; Hill, D. H. *J. Org. Chem.* **1995**, *60*, 1066–1069. (b) Percec, V.; Golding, G. M.; Smidrkal, J.; Weichold, O. *J. Org. Chem.* **2004**, *69*, 3447–3452.  
 (21) McOmie, J. F. W.; Watts, M. L.; West, D. E. *Tetrahedron* **1968**, *24*, 2289–2292.  
 (22) Tsao, M. U. *J. Am. Chem. Soc.* **1951**, *73*, 5495–5496.  
 (23) (a) Amedio, J. C., Jr.; Sunay, U. B.; Repic, O. *Synth. Commun.* **1995**, *25*, 667–680. (b) Lawrence, N. J.; Hepworth, L. A.; Rennison, D.; McGown, A. T.; Hadfield, J. A. *J. Fluorine Chem.* **2003**, *123*, 101–108.  
 (24) Wolfe, J. P.; Singer, R. A.; Yang, B. H.; Buchwald, S. L. *J. Am. Chem. Soc.* **1999**, *121*, 9550–9561.  
 (25) Percec, V.; Heck, J. J. *Polym. Sci., Part A: Polym. Chem.* **1991**, *29*, 591–597.

Scheme 3. Synthesis of AB<sub>4</sub> DendronsScheme 4. Synthesis of AB<sub>5</sub> Dendrons

assembles into a supramolecular column that self-organizes into a simple rectangular columnar  $\Phi_{r-c}$  liquid crystal lattice. (AB<sub>4</sub>)-12G2-CH<sub>2</sub>OH (39) generates a tapered conformation that mediates the formation of a centered rectangular columnar  $\Phi_{r-c}$  periodic array. (4-AB<sub>4</sub>)12G2-CO<sub>2</sub>CH<sub>3</sub> (31) adopts tapered conformations that self-assemble, depending on temperature, into helical pine-tree-like columns,<sup>6k,26</sup> forming a hexagonal columnar  $\Phi_h$  array, or untilted columns that self-organize into a  $\Phi_{r-c}$

phase. The replacement of X = CO<sub>2</sub>CH<sub>3</sub> at the apex of (4-AB<sub>4</sub>)12G2-X with X = CH<sub>2</sub>OH (40) changes the conformation of the dendron from a taper to a truncated cone (Scheme 5) and the shape of the supramolecular dendrimer from a pine-tree-like helical column to a sphere with a less densely packed center. Only the as-prepared (4-AB<sub>4</sub>)12G2-CH<sub>2</sub>OH (40) assembles into a rectangular lattice that changes irreversibly during heating into the  $Pm\bar{3}n$  cubic lattice generated from spheres with less densely packed centers. Reversible shape changes mediated by the functional group at the apex of the dendron were reported previously.<sup>7b</sup> However, this represents the first example of the transformation of a supramolecular nonporous column to a sphere with a less dense center that is mediated by the apex functionality.

(3,4-AB<sub>4</sub>)12G3-CO<sub>2</sub>CH<sub>3</sub> (32) exhibits a tapered conformation that mediates the assembly of pine-tree-like,  $\Phi_h$  assemblies. The major difference between the pine-tree-like columns assembled from (3,4-AB<sub>4</sub>)12G3-CO<sub>2</sub>CH<sub>3</sub> (32) and (4-AB<sub>4</sub>)12G2-CO<sub>2</sub>CH<sub>3</sub> (31) is in the number of tapered dendrons ( $\mu$ ) forming the column cross section. The observed trend is in line with the increased dendron dimensions and solid angle that mediate the transition from  $\mu = 3$  for (4-AB<sub>4</sub>)12G2-CO<sub>2</sub>CH<sub>3</sub> (31) to  $\mu = 2$  for (3,4-AB<sub>4</sub>)12G3-CO<sub>2</sub>CH<sub>3</sub> (32). The other remarkable feature of the pine-tree supramolecular columns is their very

(26) (a) Kwon, Y. K.; Chvalun, S.; Schneider, A. I.; Blackwell, J.; Percec, V.; Heck, J. A. *Macromolecules* **1994**, *27*, 6129–6132. (b) Kwon, Y. K.; Chvalun, S.; Blackwell, J.; Percec, V.; Heck, J. A. *Macromolecules* **1995**, *28*, 1552–1558. (c) Percec, V.; Rudick, J. G.; Peterca, M.; Wagner, M.; Obata, M.; Mitchell, C. M.; Cho, W.-D.; Balagurusamy, V. S. K.; Heiney, P. A. *J. Am. Chem. Soc.* **2005**, *127*, 15257–15264. (d) Percec, V.; Aqad, E.; Peterca, M.; Rudick, J. G.; Lemon, L.; Ronda, J. C.; De, B. B.; Heiney, P. A.; Meijer, E. W. *J. Am. Chem. Soc.* **2006**, *128*, 16365–16372.

**Scheme 5.** Self-Assembly and Structural and Retrostructural Analysis of 2-D Interdigitated Smectic A ( $S_{Ad}$ ),  $p2mm$  Simple Rectangular Columnar ( $\Phi_{r-s}$ ),  $c2mm$  Centered Rectangular Columnar ( $\Phi_{r-c}$ ), Various  $p6mm$  Hexagonal Columnar ( $\Phi_h$ ), and 3-D  $la3d$  Bicontinuous Cubic, 12-Fold Quasi-Liquid Crystal (QLC),  $Pm\bar{3}n$  Cubic (Cub),  $P4_2/mnm$  Tetragonal (Tet), and  $Im\bar{3}m$  Cubic (Cub) Lattices

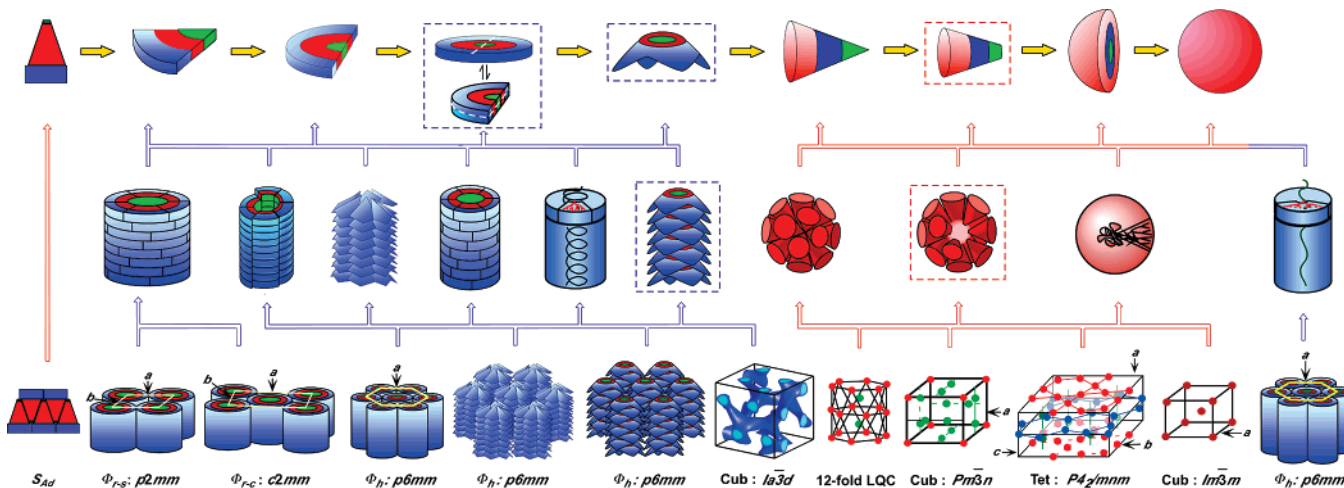


**Table 1.** Thermal Transitions of  $AB_4$ -Based Supramolecular Dendrimers

dendron	MW	thermal transitions ( $^{\circ}C$ ) and corresponding enthalpy changes (kcal/mol) <sup>a</sup>	
		heating	cooling
( $AB_4$ )12G2-CO <sub>2</sub> CH <sub>3</sub>	1143.79	$\Phi_{r-s}^k$ 74 (19.40) i $\Phi_{r-s}^k$ 74 (19.53) i	i 46 (18.94) $\Phi_{r-s}^k$
( $AB_4$ )12G2-CH <sub>2</sub> OH	1115.78	$\Phi_{r-c}^k$ 69 (18.90) i $\Phi_{r-c}^k$ 62 (18.00) i	i 41 (19.26) $\Phi_{r-c}^k$
(4- $AB_4$ )12G2-CO <sub>2</sub> CH <sub>3</sub>	1568.28	$\Phi_{r-c}^k$ 99 (24.22) i $\Phi_{h(g)}$ 27 $\Phi_h$ 82 (-20.26) $\Phi_{r-c}^k$ 100 (24.38) i	i 83 (2.54) $\Phi_h$ 23 $\Phi_{h(g)}$
(4- $AB_4$ )12G2-CH <sub>2</sub> OH	1540.27	$\Phi_r^k$ 72 (8.54) $\Phi_r$ 90 (3.26) X 97 (3.45) i $Pm\bar{3}n$ 90 (5.36) i	i 87 (5.21) $Pm\bar{3}n$
(3,4- $AB_4$ )12G3-CO <sub>2</sub> CH <sub>3</sub>	2305.55	$\Phi_{h(g)}^{io}$ 39 $\Phi_{h(g)}^{io}$ 69 (17.29) $\Phi_h$ 93 (1.59) i $\Phi_h^{io}$ 53 (5.04) $\Phi_h$ 93 (1.55) i	i 90 (1.52) $\Phi_h$ 43 (4.40) $\Phi_h^{io}$
(3,4,5- $AB_4$ )12G3-CO <sub>2</sub> CH <sub>3</sub>	3042.82	$Pm\bar{3}n(g)$ 29 $Pm\bar{3}n$ 69 (0.86) i $Pm\bar{3}n(g)$ 13 $Pm\bar{3}n$ 69 (0.83) i	i 58 (0.41) $Pm\bar{3}n$ 9 $Pm\bar{3}n(g)$
(4-3,4- $AB_4$ )12G3-CO <sub>2</sub> CH <sub>3</sub>	3154.53	g 35 X 89 (8.17) $Pm\bar{3}n$ 174 (5.04) i $Pm\bar{3}n(g)$ 58 $Pm\bar{3}n$ 173 (4.85) i	i 171 (8.07) $Pm\bar{3}n$ 41 $Pm\bar{3}n(g)$
(4-3,4- $AB_4$ )12G3-CH <sub>2</sub> OH	3126.52	g 38 X 86 (6.80) $Pm\bar{3}n$ 188 (10.74) i $Pm\bar{3}n(g)$ 56 $Pm\bar{3}n$ 184 (10.60) i	i 182 (11.03) $Pm\bar{3}n$ 56 $Pm\bar{3}n(g)$
(4-3,4,5- $AB_4$ )8G3-CO <sub>2</sub> CH <sub>3</sub>	3643.01	$\Phi_h^k$ 53 (1.92) 66 (-0.32) $\Phi_h^{io}$ $\Phi_h$ 98 (0.83) i $\Phi_{h(g)}^{io}$ 57 $\Phi_h^{io}$ $\Phi_h$ 98 (0.98) i	i 90 (1.12) $\Phi_h^{io}$ 56 $\Phi_{h(g)}^{io}$
(4-3,4,5- $AB_4$ )12G3-CO <sub>2</sub> CH <sub>3</sub>	4316.29	$\Phi_{h(g)}^{io}$ 45 (0.05) g 64 (1.49) $\Phi_h^{io}$ 70 (0.04) $\Phi_h$ 103 (0.84) i $\Phi_{h(g)}^{io}$ 45 (0.03) g 59 $\Phi_h^{io}$ 79 (0.45) $\Phi_h$ 103 (0.89) i	i 96 (1.28) $\Phi_h$ 59 g
(4-3,4,5- $AB_4$ )16G3-CO <sub>2</sub> CH <sub>3</sub>	4989.56	$\Phi_h^k$ 23 (37.79) $\Phi_h^{io}$ 71 (-0.62) $\Phi_h$ 96 (0.77) i $\Phi_h^k$ 28 (38.84) $\Phi_h^{io}$ 77 (0.75) $\Phi_h$ 96 (0.86) <sup>b</sup> i	i 87 (1.69) $\Phi_h^{io}$ 24 (40.82) $\Phi_h^k$
(4-3,4,5- $AB_4$ )12G3-CH <sub>2</sub> OH	4288.28	$\Phi_{h(g)}^{io}$ 61 (1.71) $\Phi_h^{io}$ 86 (0.71) $Pm\bar{3}n$ 140 (0.80) i <sup>c</sup>	
(4-3,4,5- $AB_4$ )12G3-CO <sub>2</sub> H	4378.31	$Pm\bar{3}n(g)$ 74 $Pm\bar{3}n$ 164 (6.40) i <sup>c</sup>	
(4-3,4,5- $AB_4$ )12G3-CH <sub>2</sub> OAc	4330.31	$\Phi_{h(g)}^{io}$ 56 (0.97) 67 (-0.51) $\Phi_h^{io}$ 97 (0.88) i	i 88 (1.13) $\Phi_h$ 50 $\Phi_{h(g)}^{io}$
(4-3,4,5- $AB_4$ )dm8G3-CO <sub>2</sub> CH <sub>3</sub>	3979.65	$Pm\bar{3}n(g)$ 58 $Pm\bar{3}n$ 131 (0.84) i $Pm\bar{3}n(g)$ 50 $Pm\bar{3}n$ 131 (0.85) i	i 120 (0.55) 110 (0.15) $Pm\bar{3}n$ 46 $Pm\bar{3}n(g)$
(4-3,4,5- $AB_4$ )dm8G3-CH <sub>2</sub> OH	3951.64	$Pm\bar{3}n(g)$ 58 $Pm\bar{3}n$ 134 (0.94) i $Pm\bar{3}n(g)$ 46 $Pm\bar{3}n$ 133 (0.98) i	i 124 (0.66) 114 (0.14) $Pm\bar{3}n$ 46 $Pm\bar{3}n(g)$

<sup>a</sup> Data from the first heating and cooling scans are on the first line, and data from the second heating are on the second line. <sup>b</sup> Enthalpy change based on overlapped peaks. <sup>c</sup> Decomposition after first heating. g = glass;  $\Phi_{r-c}$  =  $c2mm$  centered rectangular columnar lattice;  $\Phi_{r-s}$  =  $p2mm$  simple rectangular columnar lattice;  $\Phi_h$  =  $p6mm$  hexagonal columnar lattice;  $\Phi_{h(g)}$  = glassy hexagonal columnar lattice;  $\Phi_{h(g)}^{io}$  = glassy hexagonal columnar lattice with intracolumnar order;  $\Phi_h^k$  = hexagonal columnar crystal lattice;  $\Phi_h^{io}$  = hexagonal columnar lattice with intracolumnar order;  $Pm\bar{3}n$  = cubic lattice;  $Pm\bar{3}n(g)$  = glassy cubic lattice; i = isotropic; X = unknown lattice.

large tilt angle that, in both cases, is about  $45^{\circ}$ . This provides columns with relatively small diameters ( $D \cong 45 \text{ \AA}$ ). (3,4,5- $AB_4$ )12G3-CO<sub>2</sub>CH<sub>3</sub> (33) adopts a conical conformation that assembles into a supramolecular sphere. This trends agrees with that observed in previous libraries.<sup>6m,7b</sup>

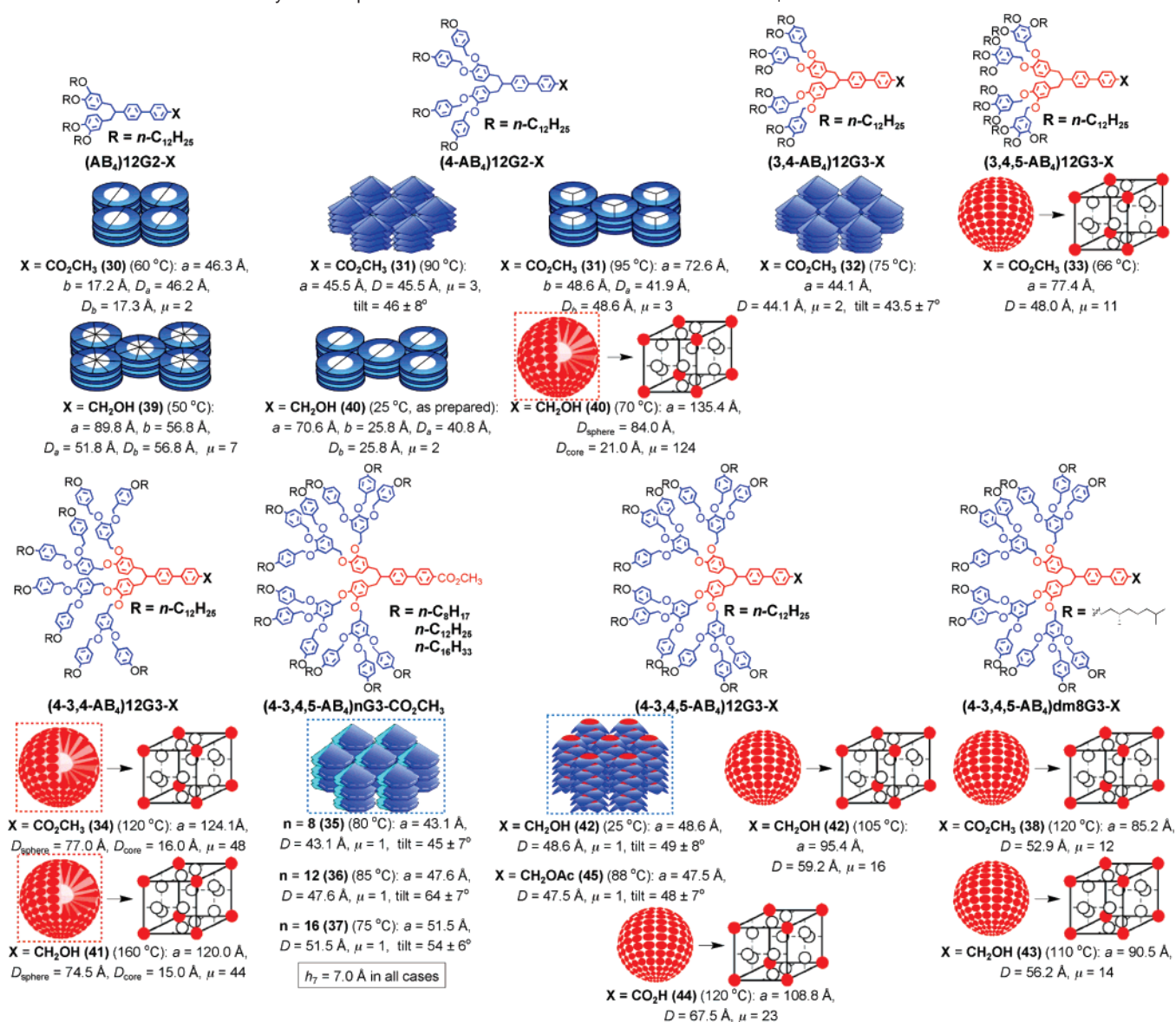
The replacement of the 3,4,5-trisubstituted benzyl ether from the periphery of the  $AB_4$  dendron with the 4-3,4-disubstituted dendron produces the transition from a conical dendron forming a supramolecular sphere to a truncated, conical dendron forming

a supramolecular sphere with a less dense center for both X = CO<sub>2</sub>CH<sub>3</sub> and CH<sub>2</sub>OH. This is an unexpected result. The supramolecular spheres with less dense centers self-assembled from (4- $AB_4$ )12G2-CH<sub>2</sub>OH (39) and (4-3,4- $AB_4$ )12G3-X with X = CO<sub>2</sub>CH<sub>3</sub> (34) and X = CH<sub>2</sub>OH (41) may provide, upon additional design refinement, pathways to hollow supramolecular dendrimers or dendritic capsules that would become complementary in structure and function to the dendritic box concept elaborated by Meijer.<sup>27</sup>

**Table 2.** Thermal Transitions of AB<sub>5</sub>-Based Supramolecular Dendrimers

dendron	MW	thermal transitions (°C) and corresponding enthalpy changes (kcal/mol) <sup>a</sup>	
		heating	cooling
(AB <sub>5</sub> )12G2-CO <sub>2</sub> CH <sub>3</sub>	1328.11	$\Phi_{r-s}^k$ 49 (20.67) $\Phi_{r-s}$ 57 (1.80) i $\Phi_{r-s}^k$ 50 (20.39) i	i 24 (21.47) $\Phi_{r-s}^k$
(4-AB <sub>5</sub> )12G2-CO <sub>2</sub> CH <sub>3</sub>	1858.72	X 56 (11.41) X 69 (4.44) <sup>b</sup> i $\Phi_{h(g)}^k$ 23 (1.13) $\Phi_h$ 69 (1.14) i	i 68 (1.10) $\Phi_h^k$ 13 $\Phi_{h(g)}^k$
(3,4-AB <sub>5</sub> )12G3-CO <sub>2</sub> CH <sub>3</sub>	2780.31	$\Phi_{h(g)}^{i0}$ 47 (1.74) 56 (-7.17) $\Phi_{h^{i0}}$ 91 (15.95) $\Phi_h$ 95 (1.88) i $\Phi_{h(g)}^{i0}$ 61 (-5.55) $\Phi_{h^{i0}}$ 92 (18.53) $\Phi_h$ 96 (1.43) i	i 95 (1.96) $\Phi_{h^{i0}}$ 60 (5.18) $\Phi_{h(g)}^{i0}$
(3,4,5-AB <sub>5</sub> )12G3-CO <sub>2</sub> CH <sub>3</sub>	3701.90	X 18 X 45 (0.74) <i>Pm</i> 3n 51 (-0.58) 68 (0.58) I <i>Pm</i> 3n(g) 23 <i>Pm</i> 3n 52 (-0.45) 68 (0.59) i	<i>Pm</i> 3n 10 <i>Pm</i> 3n(g)
(4-3,4-AB <sub>5</sub> )12G3-CO <sub>2</sub> CH <sub>3</sub>	3841.53	$\Phi_{h(g)}^{i0}$ 97 (0.66) $\Phi_{h^{i0}}$ 125 (1.67) 137 (1.62) $\Phi_{h^{i0}}$ 178 (2.29) i <sup>c</sup>	
(4-3,4,5-AB <sub>5</sub> )12G3-CO <sub>2</sub> CH <sub>3</sub>	5293.73	$\Phi_{h(g)}^{i0}$ 77 (-1.09) $\Phi_{h^{i0}}$ 125 (1.44) i $\Phi_{h(g)}^{i0}$ 82 $\Phi_{h^{i0}}$ 125 (1.46) i	i 121 (1.92) $\Phi_{h^{i0}}$ 75 $\Phi_{h(g)}^{i0}$

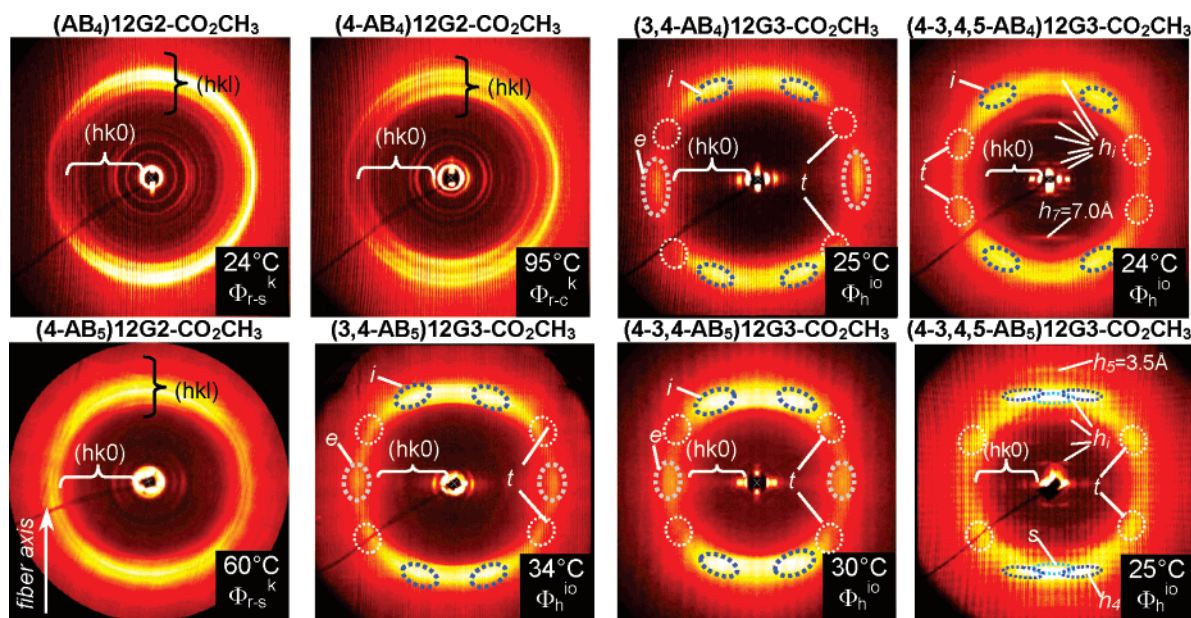
<sup>a</sup> Data from the first heating and cooling scans are on the first line, and data from the second heating are on the second line. <sup>b</sup> Enthalpy change based on overlapped peaks. <sup>c</sup> Decomposition after first heating.  $\Phi_{r-s}$  = *p2mm* simple rectangular columnar lattice;  $\Phi_{r-s}^k$  = *p2mm* simple rectangular columnar crystal lattice;  $\Phi_h$  = *ρ6mm* hexagonal columnar lattice;  $\Phi_{h(g)}^k$  = glassy hexagonal columnar crystal lattice;  $\Phi_h^k$  = hexagonal columnar crystal lattice;  $\Phi_{h(g)}^{i0}$  = glassy hexagonal columnar lattice with intracolumnar order;  $\Phi_{h^{i0}}$  = hexagonal columnar lattice with intracolumnar order; X = unknown lattice; *Pm*3n = cubic lattice; *Pm*3n(g) = glassy cubic lattice; i = isotropic.

**Scheme 6.** Retrostructural Analysis of Supramolecular Dendrimers Self-Assembled from AB<sub>4</sub> Dendrons<sup>a</sup>

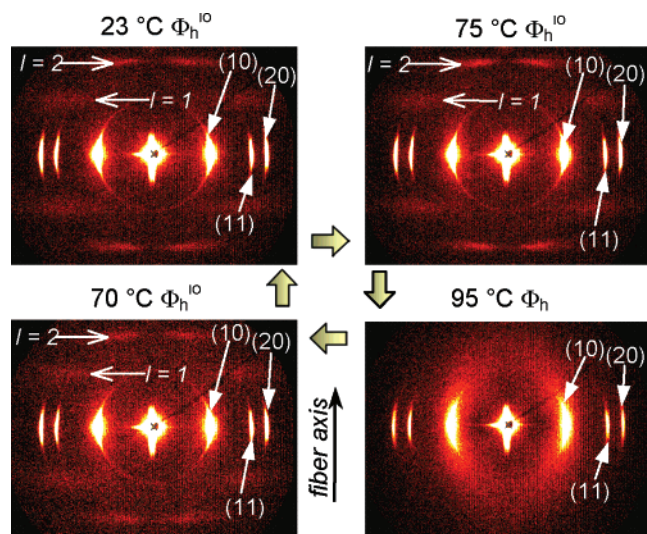
<sup>a</sup> New structures are marked with dotted rectangles.

(4-3,4,5-AB<sub>4</sub>)nG3-CO<sub>2</sub>CH<sub>3</sub>, with n = 8 (35), 12 (36), and 16 (37), shows another unexpected result. These dendrons self-

assemble into pine-tree-like helical columns that self-organize into  $\Phi_h$  and 2-D  $\Phi_h$  with intracolumnar order ( $\Phi_{h^{i0}}$ ) (Figures

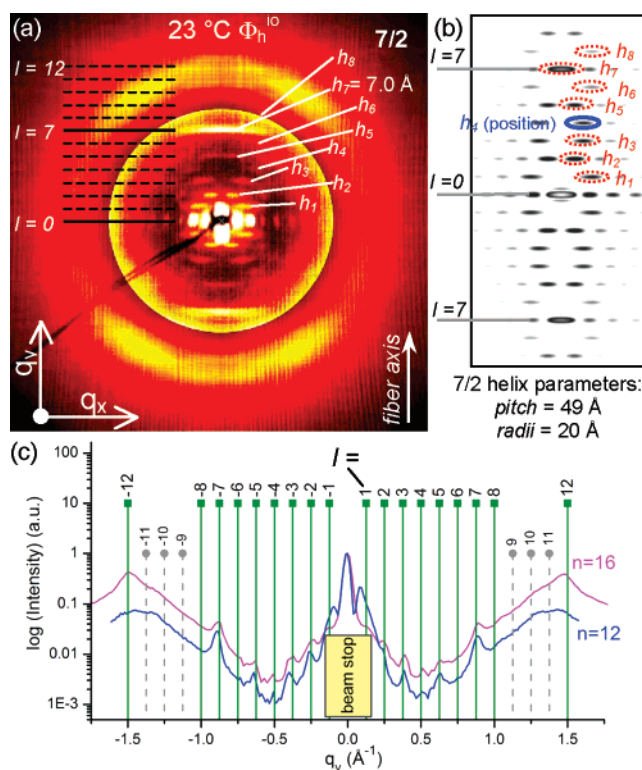


**Figure 1.** Wide-angle X-ray diffraction fiber patterns for the columnar phases of selected AB<sub>4</sub> and AB<sub>5</sub> dendrons. Recording temperatures and phases are indicated. Key: (hk0), (hk0) diffraction peaks; (hkl), (hkl) diffraction peaks observed for the ordered phases; *i*, 4.7 Å short-range helical feature [the correlation length,  $\xi = 2\pi/(\text{full width half-maximum})$ , for the  $\Phi_h$  phases  $\xi \approx 3$  column strata and for the  $\Phi_h^{io}$  phases  $\xi > 6$  column strata]; *e*,  $\sim 4.6$  Å diffuse equatorial feature; *t*, dendron tilt features; *h<sub>i</sub>*, long-range helical features indexed to a 7/2 helix observed for the (4-3,4,5-AB<sub>4</sub>)*n*G3-CO<sub>2</sub>CH<sub>3</sub> (35–37) dendrons (correlation length  $\xi > 46$  column strata, that is, larger than three full helix turns) and to a 5/1 helix packing for the (4-3,4,5-AB<sub>5</sub>)12G3-CO<sub>2</sub>CH<sub>3</sub> (51) dendron ( $\xi > 40$  column strata, that is, larger than eight full helix turns); *s*, 4.4 Å stacking along the column axis feature.



**Figure 2.** Small-angle XRD fiber patterns for the reversible  $\Phi_h$ – $\Phi_h^{io}$  transition of the (4-3,4,5-AB<sub>4</sub>)12G3-CO<sub>2</sub>CH<sub>3</sub> (36) dendron. The scan temperatures, (10), (11), and (20) diffraction peaks of the  $\Phi_h$ , and the first two ( $l = 1, 2$ ) helical layer lines are indicated.

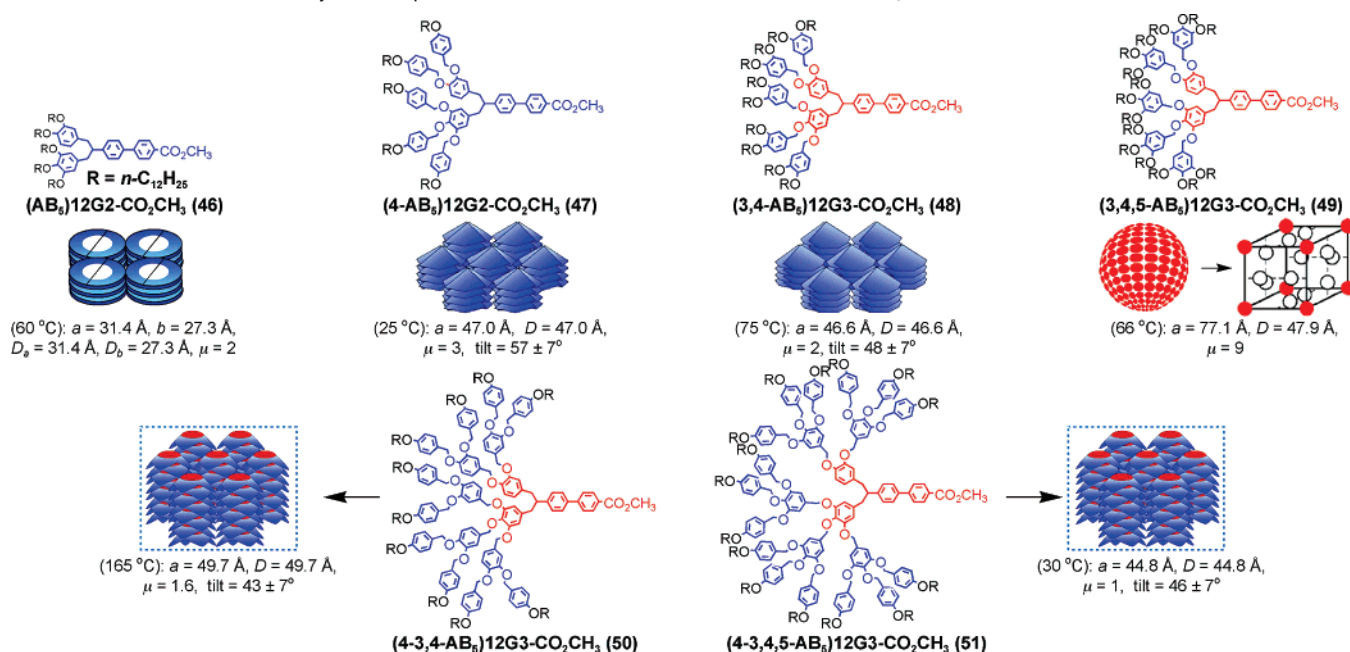
1 and 2, Supporting Figures SF4 and SF5). However, the investigation of the wide-angle XRD aligned fiber patterns of all hexagonal periodic arrays assembled from the AB<sub>4</sub>-based dendrons indicates that (4-3,4,5-AB<sub>4</sub>)*n*G3-CO<sub>2</sub>CH<sub>3</sub>, with  $n = 8$  (35), 12 (36), and 16 (37), display a 7.0 Å ( $h_7$  in Figure 1 and SF4) repeat unit along the long axis of the column, generated from a single dendron ( $\mu = 1$ ) forming the cross section of the column. This contrasts the 4.7 Å repeat unit along the column long axis that is most commonly encountered for conventional tapered dendrons.<sup>7b</sup> This dependence between  $\mu = 1$  and  $h_7 = 7.0$  Å can be explained only by an intramolecular back-folding of a disc-like dendron into a half-disc, tapered dendron with double thickness (Schemes 5 and 6).



**Figure 3.** (a) (4-3,4,5-AB<sub>4</sub>)*n*G3-CO<sub>2</sub>CH<sub>3</sub> (36) wide-angle XRD fiber pattern for  $n = 12$ ; the central region of the pattern is overlaid with higher contrast. (b) Simulation of an ideal 7/2 helix fiber pattern. (c)  $q_y$  plots for  $n = 12$  and 16; the observed helical layer lines are indicated. The red dotted circles in (b) indicate the agreement in intensity and position of  $h_i$  helical features (layer lines = principal maxima); the filled blue circle in (b) shows the disagreement of the fourth layer maximum position.

The helical diffraction theory<sup>28a,b</sup> has been used for the analysis of the most basic helical biological macromolecules, such as polypeptides,<sup>28c</sup> DNA,<sup>28d–f</sup> tobacco mosaic virus,<sup>28g</sup> and



**Scheme 7.** Retrostructural Analysis of Supramolecular Dendrimers Self-Assembled from AB<sub>5</sub> Dendrons<sup>a</sup>

<sup>a</sup> New structures are marked with dotted rectangles.

collagen,<sup>28h</sup> from fiber XRD experiments. Here, we have applied for the first time the helical diffraction theory to the structural analysis of helical supramolecular dendrimers. For details, see the Supporting Information.

By using the helical diffraction theory, a pine-tree-like helical supramolecular column with a long-range  $7/2$  helix, with length longer than 46 column strata or more than three full helix turns, was demonstrated for the structures assembled from **(4-3,4,5-AB<sub>4</sub>)*n*G3-CO<sub>2</sub>CH<sub>3</sub>**, with  $n = 8$  (**35**), 12 (**36**), and 16 (**37**), via the new back-folded dendritic conformation with double thickness (Figure 3). More details about this structure and its self-assembly mechanism are discussed in a later section.

The replacement of  $X = \text{CO}_2\text{CH}_3$  (**36**) with  $X = \text{CH}_2\text{OH}$  (**42**) in **(4-3,4,5-AB<sub>4</sub>)12G3-X** eliminates the back-folding mechanism of the disc-like dendron, and the disc-like dendron tilts into an unprecedented crown-like conformation that assembles into helical pyramidal columns resembling those generated from conformationally restricted crown-like conformations.<sup>29</sup> At higher temperatures, these pyramidal columns change their shape into supramolecular spheres. The mechanism of this structural transformation is not yet known. However, the generality of the dendritic crown-like conformation, the mechanism of this

supramolecular shape change, and the new functions generated by this novel supramolecular concept are under investigation and will be reported soon. **(4-3,4,5-AB<sub>4</sub>)12G3-CO<sub>2</sub>H** (**44**) assembles only into supramolecular spheres, while **(4-3,4,5-AB<sub>4</sub>)12G3-CH<sub>2</sub>OAc** (**45**) self-assembles only into pyramidal columns, most probably via a crown-like dendron conformation. Attempts to investigate the transfer of stereochemical information in the long-range helical columns assembled from **(4-3,4,5-AB<sub>4</sub>)12G3-CO<sub>2</sub>CH<sub>3</sub>** (**36**) by incorporating stereocenters on their alkyl tails yielded **(4-3,4,5-AB<sub>4</sub>)dm8G3-X**, with  $X = \text{CO}_2\text{CH}_3$  (**38**) and  $\text{CH}_2\text{OH}$  (**43**) (Schemes 3 and 6). Unfortunately, these dendrons self-assemble into supramolecular spheres rather than into long-range helical pine-tree-like columns.

**Structural and Retrostructural Analysis of the AB<sub>5</sub> Library.** The transition from the hybrid symmetric AB<sub>4</sub> dendron to the hybrid asymmetric AB<sub>5</sub> dendron (Schemes 1 and 2) was investigated with five examples of self-assembling dendrons (Scheme 7). Some similarities and significant differences were observed. For example, **(AB<sub>5</sub>)12G2-CO<sub>2</sub>CH<sub>3</sub>** (**46**) displays a distorted half-disc conformation similar to that of **(AB<sub>4</sub>)12G2-CO<sub>2</sub>CH<sub>3</sub>** (**30**). **(4-AB<sub>5</sub>)12G2-CO<sub>2</sub>CH<sub>3</sub>** (**47**) also displays a tapered conformation related to that of **(4-AB<sub>4</sub>)12G2-CO<sub>2</sub>CH<sub>3</sub>** (**31**). In both cases, the tapered dendron assembles into pine-tree-like columns with similar dimensions. These pine-tree-like columns self-organize into  $\Phi_h$  periodic arrays. However, the  $\Phi_h$  lattice generated from **(4-AB<sub>5</sub>)12G2-CO<sub>2</sub>CH<sub>3</sub>** (**47**) lacks the polymorphism of the structure assembled from **(4-AB<sub>4</sub>)12G2-CO<sub>2</sub>CH<sub>3</sub>** (**31**). **(3,4-AB<sub>5</sub>)12G3-CO<sub>2</sub>CH<sub>3</sub>** (**48**) assembles into a pine-tree-like column similar to **(3,4-AB<sub>4</sub>)12G3-CO<sub>2</sub>CH<sub>3</sub>** (**32**), while **(3,4,5-AB<sub>5</sub>)12G3-CO<sub>2</sub>CH<sub>3</sub>** (**49**) assembles into a supramolecular sphere related to that produced from **(3,4,5-AB<sub>4</sub>)12G3-CO<sub>2</sub>CH<sub>3</sub>** (**33**).

The most striking difference is observed in the case of **(4-3,4-AB<sub>5</sub>)12G3-CO<sub>2</sub>CH<sub>3</sub>** (**50**). This dendron forms a pyramidal column, while its AB<sub>4</sub> counterpart **(4-3,4-AB<sub>4</sub>)12G3-CO<sub>2</sub>CH<sub>3</sub>**

- (27) (a) Jansen, J. F. G. A.; de Brabander-van den Berg, E. M. M.; Meijer, E. W. *Science* **1994**, *266*, 1226–1229. (b) Jansen, J. F. G. A.; Meijer, E. W.; de Brabander-van den Berg, E. M. M. *J. Am. Chem. Soc.* **1995**, *117*, 4417–4418.
- (28) (a) Cochran, W.; Crick, F. H. C.; Vand, V. *Acta Crystallogr.* **1952**, *5*, 581–586. (b) Klug, A.; Crick, F. H. C.; Wyckoff, H. W. *Acta Crystallogr.* **1958**, *11*, 199–213. (c) Cochran, W.; Crick, F. H. C. *Nature* **1952**, *169*, 234–235. (d) Wilkins, M. H. F.; Stokes, A. R.; Wilson, H. R. *Nature* **1953**, *171*, 738–740. (e) Franklin, R. E.; Gosling, R. G. *Nature* **1953**, *171*, 740–741. (f) Klug, A. *J. Mol. Biol.* **2004**, *335*, 3–26. (g) Franklin, R. E.; Klug, A. *Acta Crystallogr.* **1955**, *8*, 777–780. (h) Cohen, C.; Bear, R. S. *J. Am. Chem. Soc.* **1953**, *75*, 2783–2784.
- (29) (a) Zimmermann, H.; Poupko, R.; Luz, Z.; Billard, J. Z. *Naturforsch., A: Phys. Sci.* **1985**, *40*, 149–160. (b) Malthête, J.; Collet, A. *Nouv. J. Chim.* **1985**, *9*, 151–153. (c) Levelut, A. M.; Malthête, J.; Collet, A. *J. Phys.* **1986**, *47*, 351–357. (d) Malthête, J.; Collet, A. *J. Am. Chem. Soc.* **1987**, *109*, 7544–7545. (e) Poupko, R.; Luz, Z.; Spielberg, N.; Zimmermann, H. *J. Am. Chem. Soc.* **1989**, *111*, 6094–6105. (f) Luz, Z.; Poupko, R.; Wachtel, E. J.; Zimmermann, H.; Bader, V. *Mol. Cryst. Liq. Cryst.* **2003**, *397*, 367–377.

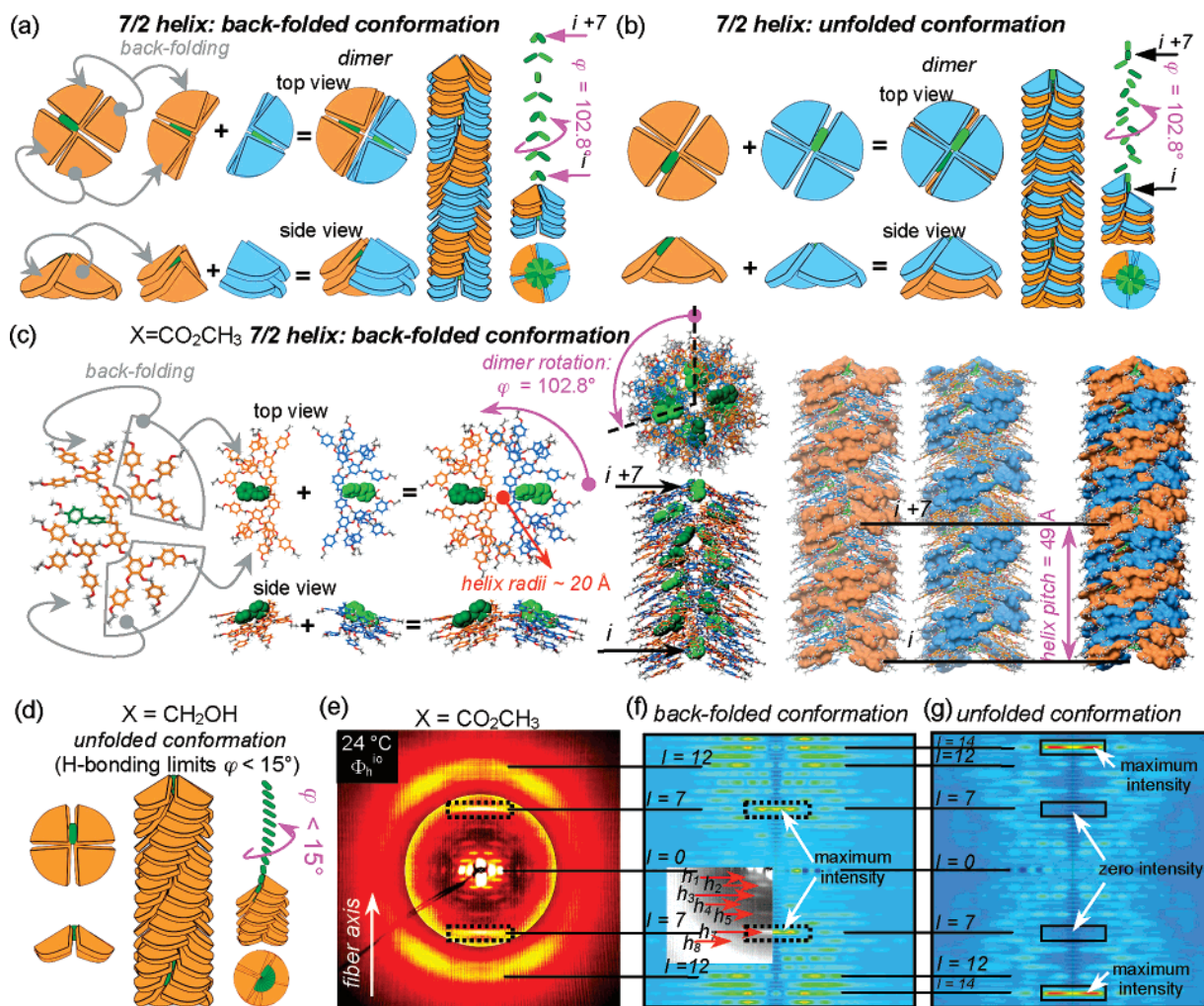


**Figure 4.** Schematic of the self-assembly of (4-3,4,5-AB<sub>4</sub>)nG3-X into supramolecular pine-tree-like columns (a) with and (b,d) without back-folding; molecular model for the dendrons with X = CO<sub>2</sub>CH<sub>3</sub> (35–37) (c); and fiber patterns for the dendron (4-3,4,5-AB<sub>4</sub>)12G3-X, with X = CO<sub>2</sub>CH<sub>3</sub> (36), (e) collected and (f,g) simulated by using Cerius2 software. In (c), the 7/2 helix parameters are indicated: from left to right, schematic of the self-folding, dimer structure, top and side stick views, and side surface views of the supramolecular pine-tree-like columns. Color code: the biphenyl at the apex of the AB<sub>4</sub> dendron is colored green; the aromatic and benzyl regions of the dendron are colored in orange or blue, respectively.

(34) generates a sphere with low density in the center. Another interesting difference is observed for the case of (4-3,4,5-AB<sub>5</sub>)-12G3-CO<sub>2</sub>CH<sub>3</sub> (51), whose most probable conformation is crown-like, while the disc-like conformation of (4-3,4,5-AB<sub>4</sub>)-12G3-CO<sub>2</sub>CH<sub>3</sub> back-folds intramolecularly into a half-disc taper with double thickness.

**The Intramolecular Back-Folded Tapered Model with Double Thickness of (4-3,4,5-AB<sub>4</sub>)nG3-CO<sub>2</sub>CH<sub>3</sub>.** The top line of Scheme 5 illustrates, from left to right, the hierarchical evolution of dendron conformation as a function of generation number. A tapered dendron increases the projection of its solid angle<sup>7b</sup> from a fragment of a disc or tapered conformation to a disc to a cone to a fragment of a sphere and subsequently reaches the shape of a sphere.<sup>6b</sup> In a previous section, (4-3,4,5-AB<sub>4</sub>)nG3-CO<sub>2</sub>CH<sub>3</sub> dendrons with  $n = 8$  (35), 12 (36), and 16 (37) were shown to change their disc-like conformation into a half-disc tapered conformation with double thickness via an intramolecular back-folding process. This back-folded structure is observed in a  $\Phi_h$  lattice with intracolumnar order ( $\Phi_{h^{io}}$ )<sup>26h-j,30c</sup> that undergoes a reversible first-order transition to a conventional 2-D  $\Phi_h$  liquid crystal phase (SF1). This reversible transition was also detected by small-angle XRD experiments performed

on oriented fibers (Figure 2). In the  $\Phi_{h^{io}}$  phase, the first two helical layer lines,  $l = 1$  and 2, of the long-range order helical conformation of the pine-tree-like column are seen. In the wide-angle XRD of the same fiber, both the helical fiber pattern and the intracolumnar double dendron spacing ( $h_7 = 7.0 \text{ \AA}$ ) are observed (Figure 3a,c).

Simulation of the helical fiber pattern from Figure 3a,c by using the helical diffraction theory<sup>28a</sup> is fitted best with a long-range 7/2 helix (Figure 3b and SF4). Theoretically, such an XRD feature can be generated by an intramolecularly back-folded structure that generates a half-disc tapered conformation with double thickness (Figure 3a,c) or by an assembly of two discs (one orange and one blue) that rotates in a cooperative way as a single repeat unit (Figure 3b). In both models, the biphenyl group of the apex of the dendron is colored green. Two back-folded dendrons colored orange and blue form a supramolecular dimer that assembles into a long-range helical structure (Figure 4a,c). When X = CO<sub>2</sub>CH<sub>3</sub> (36) from the apex of the dendron is changed to X = CH<sub>2</sub>OH (42), the conformation of the dendron changes to crown-like. This crown conformation facilitates intermolecular H-bonding along the column or intradendron H-bonding (Figure 4d, Scheme 6). Simulation of the XRD from

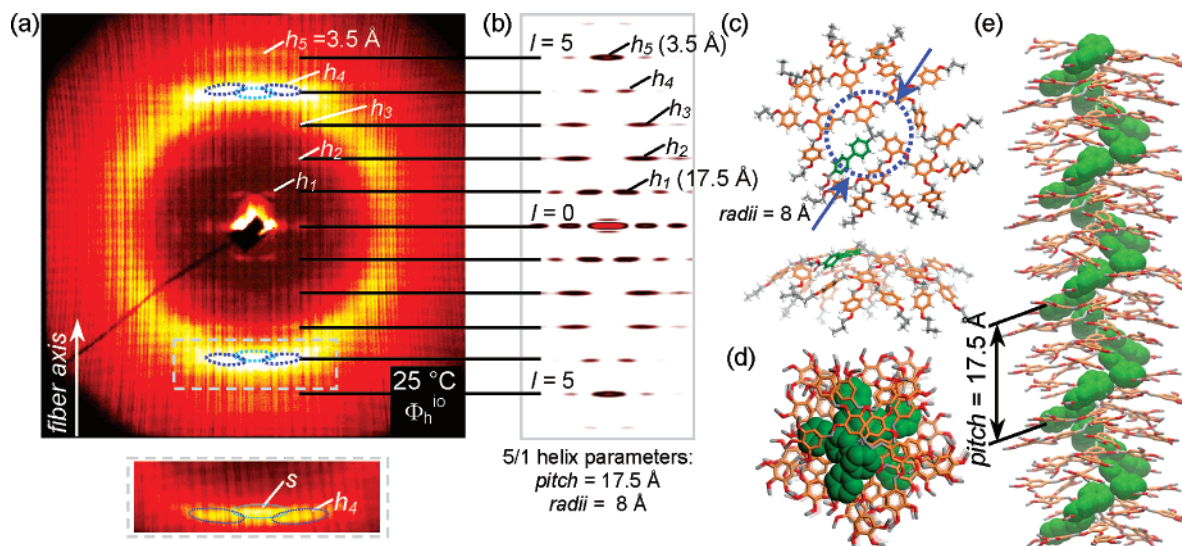


**Figure 5.** (a) Wide-angle XRD oriented fiber pattern of (4-3,4,5-AB<sub>5</sub>)12G3-CO<sub>2</sub>CH<sub>3</sub> (**51**) in the  $\Phi_{h^{10}}$  phase. The lower inset shows an enlargement of the dotted region from the fiber pattern with higher contrast. (b) Fiber pattern simulation from an ideal 5/1 helix. (c) Top and side views of the crown-like molecular model. (d) Top and (e) side views of the supramolecular helical pyramidal column (only a part of the aromatic core region is shown). In (a,b),  $h_1 \dots h_5$  are long-range helical features assigned to a 5/1 helical packing, and  $s = 4.4$  Å are stacking along the column axis features. Color code in (c–e): the biphenyl at the dendron apex is colored green; benzyl groups, orange; carbon atoms, gray; oxygen atoms, red; hydrogen atoms, white.

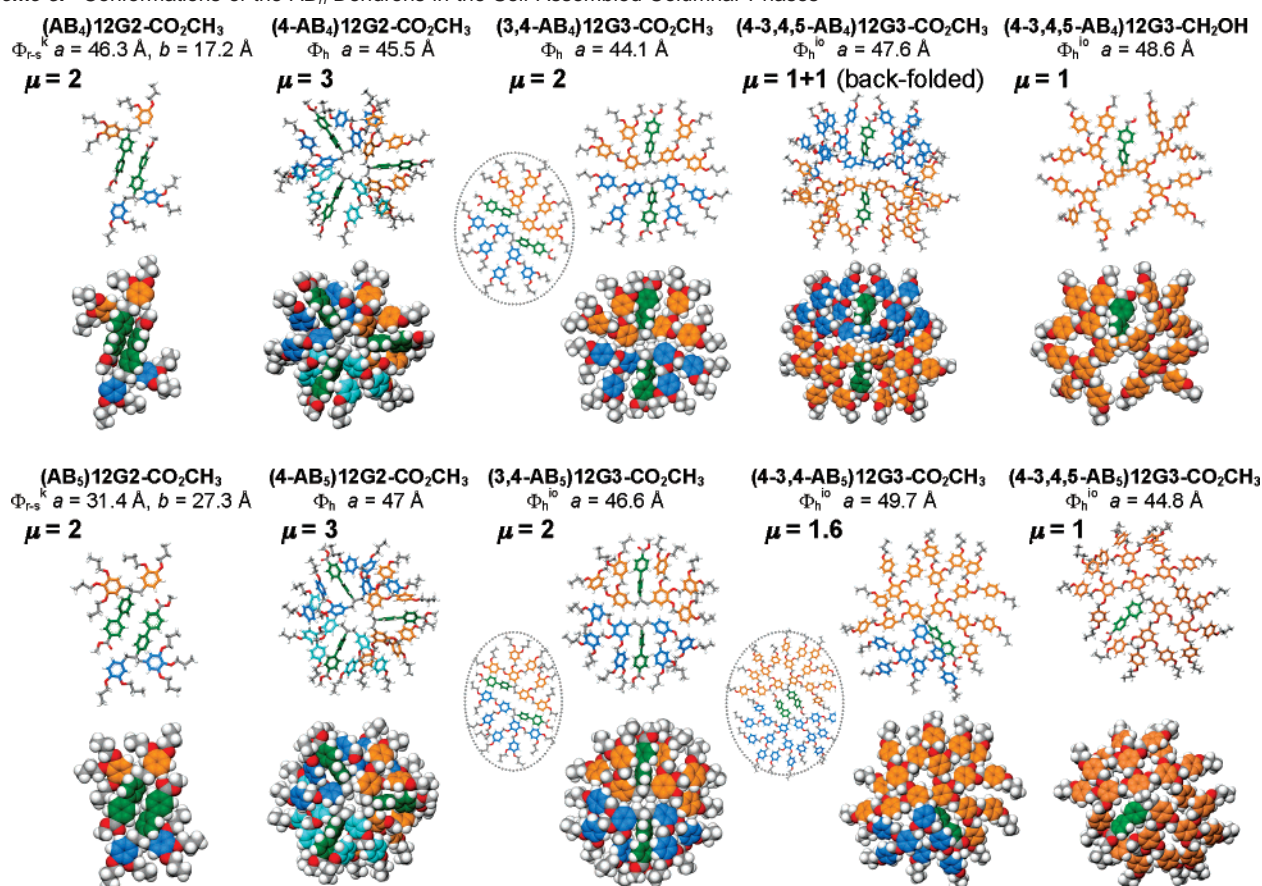
Figure 4e is matched by the intramolecular back-folded model (Figure 4a,f) but not by the alternative model based on cooperative motion of a pair of two tilted discs (Figure 4b,g). Therefore, this simulation experiment demonstrates the novel intramolecular back-folded dendron conformation from Figure 4a and eliminates the model from Figure 4b.

**Crown-like Conformation of (4-3,4,5-AB<sub>5</sub>)12G3-X, (4-3,4-AB<sub>5</sub>)12G3-X, and (4-3,4,5-AB<sub>5</sub>)12G3-X Dendrons.** The results discussed above have also suggested crown-like conformations for (4-3,4,5-AB<sub>4</sub>)12G3-X, with X = CH<sub>2</sub>OH (**42**) and CH<sub>2</sub>-OAc (**45**) (Scheme 6, Figure 4d), for (4-3,4-AB<sub>5</sub>)12G3-CO<sub>2</sub>CH<sub>3</sub> (**50**), and for (4-3,4,5-AB<sub>5</sub>)12G3-CO<sub>2</sub>CH<sub>3</sub> (**51**) (Scheme 7). The wide-angle XRD analysis of aligned fibers and the model from Figure 5, generated by using the helical diffraction theory, demonstrate the crown conformation for the case of (4-3,4,5-AB<sub>5</sub>)12G3-CO<sub>2</sub>CH<sub>3</sub> (**51**). The simulation of the fiber XRD pattern from Figure 5a with the crown conformation from Figure 5c by using the helical diffraction theory<sup>28a</sup> is best fitted by a long-range 5/1 helix that contains at least 40 column strata or 8 helix turns (Figure 5b). The 3.5 Å repeat along the pyramidal column axis generated from crown-like dendrons (Figure 5a,b) is in perfect agreement with the 7.0 Å repeat observed for the pine-tree-like columns generated from back-folded tapered dendrons (Figure 3a,b); therefore, these data support these two models. The top view and side view of the helical pyramidal column that resulted from the XRD analysis are shown in Figure 5d,e.

**Conformation of the AB<sub>4</sub> and AB<sub>5</sub> Hybrid Dendrons in the Columnar Assemblies.** In the previously reported benzyl ether self-assembling dendrons, the 3,4- and the 3,4,5-substitution pattern of the branching point mediated predominantly the assembly of supramolecular spherical dendrimers generated from the conical conformation of the dendrons.<sup>7b,10a,b</sup> The incorporation of the 3,5-substitution pattern enhances the tendency toward tapered dendron conformations that mediate the assembly of columnar structures.<sup>6n,7b,12j,30</sup> The replacement of a benzyl ether with a phenyl propyl ether repeat unit also enhances the tendency toward the assembly of columnar structures.<sup>6m</sup> Therefore, on

the basis of previous results, the replacement of an AB<sub>3</sub> building block with an AB<sub>4</sub> or AB<sub>5</sub> building block was expected to generate predominantly self-assembling dendrons that would assemble into spherical supramolecular dendrimers. Contrary to this expectation, the results summarized in Schemes 6 and 7 demonstrate that the self-assembling dendrons generated from these AB<sub>4</sub> and AB<sub>5</sub> building blocks exhibit a high tendency to generate supramolecular columns via dendron conformations that were not encountered before. This result prompted a more detailed investigation of the conformations of these hybrid dendrons during the assembly of columnar structures. The AB<sub>4</sub> building block (Schemes 1 and 6) consists of an AB<sub>2</sub>(C<sub>2</sub>)<sub>2</sub> sequence that contains a B<sub>2</sub> branching point generated from a tetrahedral carbon. The B<sub>4</sub> functionality is incorporated via two 3,4-dihydroxyphenyl groups, C<sub>2</sub>, that are attached to the tetrahedral branching point. The AB<sub>5</sub> building block (Schemes 2 and 7) consists of an AB<sub>2</sub>C<sub>2</sub>C<sub>3</sub> sequence that contains a B<sub>2</sub> tetrahedral carbon branching point, with the B<sub>5</sub> functionality incorporated via a 3,4-dihydroxyphenyl group and a 3,4,5-trihydroxyphenyl group that are both attached to the tetrahedral carbon of the B<sub>2</sub> branching point. Therefore, these sequences of two 3,4-AB<sub>2</sub> repeat units, or a 3,4-AB<sub>2</sub> and a 3,4,5-AB<sub>3</sub> repeat units, connected via a tetrahedral branching point resemble sequences of 3,4- and 3,4,5-substituted benzyl ethers with 3,5-disubstituted benzyl ethers<sup>6m,7b</sup> in which the 3,5-disubstituted benzyl ether is replaced with a conformationally more flexible tetrahedral branching point.

Scheme 8 summarizes the top views of the most representative, previously unencountered dendritic conformations that generated the columnar supramolecular structures from Schemes 6 and 7. In Scheme 8, (AB<sub>4</sub>)12G2-CO<sub>2</sub>CH<sub>3</sub> (**30**) and (AB<sub>5</sub>)-12G2-CO<sub>2</sub>CH<sub>3</sub> (**46**) are the only two self-assembling dendrons that exhibit a close to classic tapered conformation,<sup>6j,m,7b</sup> containing a tilted biphenyl group at its apex. (4-AB<sub>4</sub>)12G2-CO<sub>2</sub>CH<sub>3</sub> (**31**) and (4-AB<sub>5</sub>)12G2-CO<sub>2</sub>CH<sub>3</sub> (**47**) display the first examples of previously unencountered taper conformations, with the biphenyl from the apex being back-folded into the inner aromatic part of the taper.

**Scheme 8.** Conformations of the AB<sub>n</sub> Dendrons in the Self-Assembled Columnar Phases<sup>a</sup>

<sup>a</sup> In all cases, the biphenyl at the dendron apex is colored in green. Each dendron has its aromatic rings colored differently (blue, orange, and light blue), and for simplicity, only three methylenic units of the paraffin chains are shown. The alternative dendron conformations indicated by the dotted circles are less probable to generate a columnar hexagonal phase.

$(3,4\text{-AB}_4)_2\text{12G3-CO}_2\text{CH}_3$  (32) and  $(3,4\text{-AB}_5)_2\text{12G3-CO}_2\text{CH}_3$  (48) show the new half-disc-like conformations containing the biphenyl back-folded into the inner aromatic part of the dendron.  $(4\text{-3,4,5-AB}_4)_2\text{12G3-CO}_2\text{CH}_3$  (36) exhibits a back-folded half-disc conformation, containing the biphenyl from the apex also back-folded in the inner aromatic part of the dendron. The thickness of this back-folded dendron is approximately 2 times larger than that of the unfolded dendrons.

$(4\text{-3,4,5-AB}_4)_2\text{12G3-CH}_2\text{OH}$  (42),  $(4\text{-3,4-AB}_5)_2\text{12G3-CO}_2\text{CH}_3$  (50), and  $(4\text{-3,4,5-AB}_5)_2\text{12G3-CO}_2\text{CH}_3$  (51) exhibit crown-like conformations. The crown conformations of  $(4\text{-3,4,5-AB}_4)_2\text{12G3-CH}_2\text{OH}$  (42) and  $(4\text{-3,4,5-AB}_5)_2\text{12G3-CO}_2\text{CH}_3$  (51) cover the entire cross section of the supramolecular column. However, the crown conformation of  $(4\text{-3,4-AB}_5)_2\text{12G3-CO}_2\text{CH}_3$  (50) covers only about 63% of the column cross section, with the rest being covered by the next dendron. These new dendritic conformations were not encountered before in libraries of AB<sub>2</sub> and AB<sub>3</sub> benzyl ether dendrons.

**Supramolecular Spherical Dendrimers with a Less Dense Center.** The data summarized in Schemes 6 and 7 show that certain dendrons self-assemble into spherical supramolecular dendrimers that self-organize into  $Pm\bar{3}n$  lattices.<sup>6d,m,7b</sup> The most remarkable observation is that some of these lattices exhibit enhanced amplitudes of their higher order diffraction peaks (Figure 6). The enhanced amplitude indicates a less dense packing in the centers of columnar hexagonal and columnar rectangular<sup>6m,12j,30d</sup> lattices as well as of  $Pm\bar{3}n$  cubic lattices.<sup>6m</sup>

The XRD data from Figure 6a indicate a  $Pm\bar{3}n$  cubic lattice generated from non-hollow spheres for the case of  $(4\text{-3,4,5-AB}_4)_2\text{12G3-CH}_2\text{OH}$  (42) and a  $Pm\bar{3}n$  cubic lattice generated from spheres with less dense center for the cases of  $(4\text{-AB}_4)_2\text{12G2-CH}_2\text{OH}$  (40) and  $(4\text{-3,4-AB}_4)_2\text{12G3-CH}_2\text{OH}$  (41). A detailed analysis of the XRD of  $(4\text{-3,4-AB}_4)_2\text{12G3-CH}_2\text{OH}$  (41) is shown in Figure 6b. It is interesting to observe that the fully extended conformation of the  $(4\text{-AB}_4)_2\text{12G2-CH}_2\text{OH}$  (40) dendron is shorter than those for the  $(4\text{-3,4-AB}_4)_2\text{12G3-CH}_2\text{OH}$  (41) and  $(4\text{-3,4,5-AB}_4)_2\text{12G3-CH}_2\text{OH}$  (42) dendrons (Scheme 6). In fact, the fully extended conformations of the last two dendrons are equal. This dependence must correlate with the diameter of the supramolecular spheres resulting from their self-assembly if the structures of their supramolecular spheres are identical. However, this is not the case. The lattice dimensions of the  $Pm\bar{3}n$  cubic lattices follow the reverse trend, i.e.,  $a = 135.4 \text{ \AA}$  for  $(4\text{-AB}_4)_2\text{12G2-CH}_2\text{OH}$  (40),  $a = 120 \text{ \AA}$  for  $(4\text{-3,4-AB}_4)_2\text{12G3-CH}_2\text{OH}$  (41), and  $a = 95.4 \text{ \AA}$  for  $(4\text{-3,4,5-AB}_4)_2\text{12G3-CH}_2\text{OH}$  (42) (Figure 6a). This trend correlates with the enhanced amplitude of the XRD high-order peaks for the cases of  $(4\text{-3,4-AB}_4)_2\text{12G3-CH}_2\text{OH}$  (41) and  $(4\text{-AB}_4)_2\text{12G2-CH}_2\text{OH}$

(30) (a) Percec, V.; Dulcey, A. E.; Peterca, M.; Ilies, M.; Sienkowska, M. J.; Heiney, P. A. *J. Am. Chem. Soc.* **2005**, *127*, 17902–17909. (b) Percec, V.; Dulcey, A. E.; Peterca, M.; Ilies, M.; Nummelin, S.; Sienkowska, M. J.; Heiney, P. A. *Proc. Natl. Acad. Sci. U.S.A.* **2006**, *103*, 2518–2523. (c) Peterca, M.; Percec, V.; Dulcey, A. E.; Nummelin, S.; Korey, S.; Ilies, M.; Heiney, P. A. *J. Am. Chem. Soc.* **2006**, *128*, 6713–6720. (d) Percec, V.; Dulcey, A. E.; Peterca, M.; Adelman, P.; Samant, R.; Balagurusamy, V. S. K.; Heiney, P. A. *J. Am. Chem. Soc.* **2007**, *129*, 5992–6002.

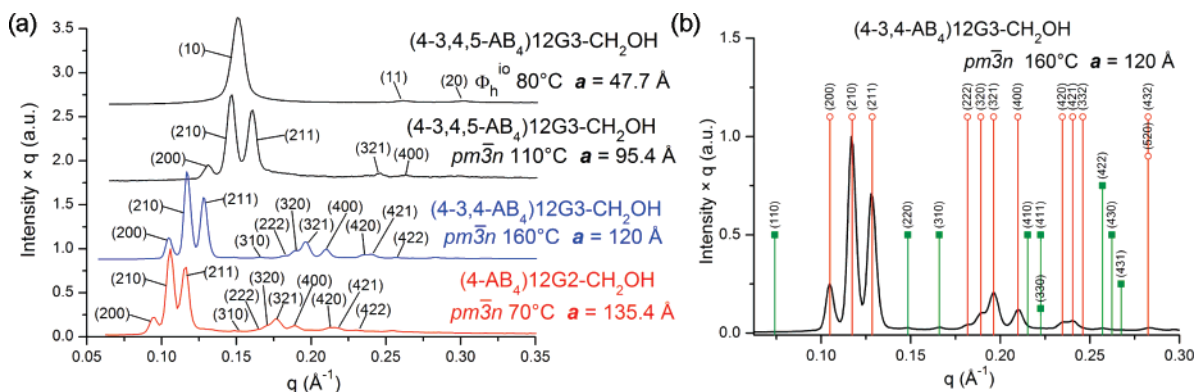


**Figure 6.** (a) Small-angle X-ray powder diffraction plots for the indicated  $AB_4$  dendrons, and (b) detailed plot for the  $(4-3,4-AB_4)12G3-CH_2OH$  (**41**). In (b), the lines indicate the agreement between the experimental and theoretical peak positions. The diffraction peaks indicated by the green lines should have zero intensity if the face and corner supramolecular assemblies are identical. The collection temperatures and lattice parameters are indicated.

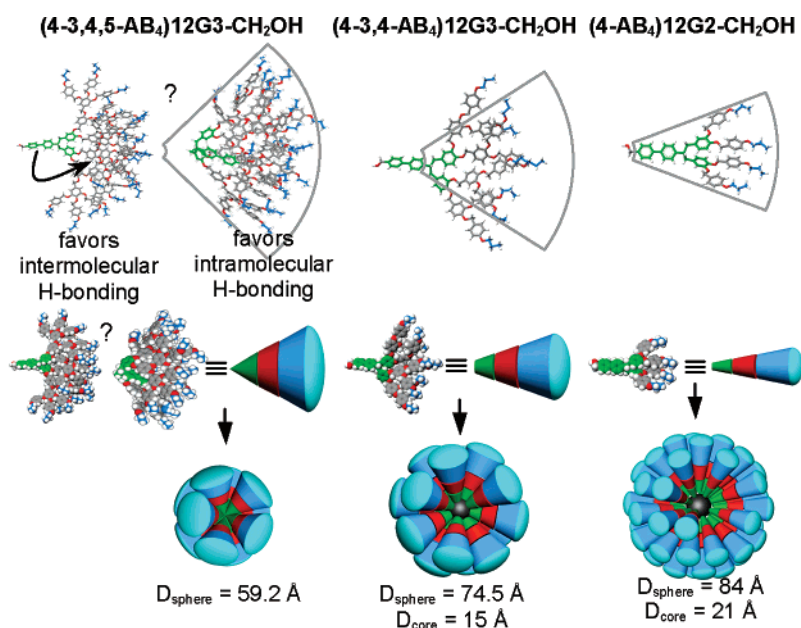


**Figure 7.** Schematic of the  $AB_4$  dendrons that self-assemble into supramolecular spherical assemblies. The various conical shapes shown suggest the correlation between dendron solid angle and sphere or less dense center diameters.

(**40**); therefore, the enhanced lattice dimension,  $a$ , is explained by an increased sphere diameter generated by a less dense center.

Figure 7 illustrates the most probable truncated conical dendron conformations that correlate with the diameter of the supramolecular sphere ( $D_{\text{sphere}}$ ) and the diameter of the less dense center of the sphere ( $D_{\text{core}}$ ). In the case of  $(4-3,4,5-AB_4)12G3-CH_2OH$  (**42**), intramolecular back-folding of the dendron and of the biphenyl apex is required to provide a conical dendron that self-assembles into a non-hollow supramolecular sphere with  $D_{\text{sphere}} = 59.2 \text{ \AA}$ . However, a non-back-folded conformation of the  $(4-3,4-AB_4)12G3-CH_2OH$  (**41**) dendrons is required to generate the truncated conical shape to provide  $D_{\text{sphere}} = 74.5 \text{ \AA}$  and  $D_{\text{core}} = 15 \text{ \AA}$ . Back-folding is also not required in the case of  $(4-AB_4)12G2-CH_2OH$  (**40**) in order to produce the truncated conical conformation that provides  $D_{\text{sphere}} = 84 \text{ \AA}$  and  $D_{\text{core}} = 21 \text{ \AA}$ . It is interesting to observe that the back-folding required to generate the cone from  $(4-3,4,5-AB_4)12G3-CH_2OH$  (**42**) is similar to that required to generate the back-folded tapered dendron from  $(4-3,4,5-AB_4)nG3-CO_2CH_3$ , with  $n = 8$  (**35**), 12 (**36**), and 16 (**37**). The values of the  $D_{\text{core}}$  from Figure 7 were calculated by adapting the previous model elaborated for the calculation of porous columns<sup>12j,30d</sup> to spheres

with less dense centers. Details of the calculation of the XRD for spheres with less dense centers or hollow centers will be reported elsewhere. The reconstruction of the electron density of the  $Pm\bar{3}n$  cubic array generated by  $(4-AB_4)12G2-CH_2OH$  (**40**) is shown in Figure 8.

The electron density data, together with the dendron conformation from Figure 7 and the dimensions from Scheme 6, were used to construct the supramolecular sphere with a less dense center shown in Figure 9. This model suggests potential design pathways for hollow supramolecular spheres that are expected to complement the dendritic box concept.<sup>27</sup>

## Conclusions

The synthesis of the first examples of  $AB_4$  and  $AB_5$  dendritic building blocks with complex architecture is reported. Both compounds were constructed by the interconnection of the A functional group to two  $B_2$  functional groups, or to a combination of  $B_2$  and  $B_3$  functional groups, via a conformationally flexible tetrahedral branching point. These building blocks are first-generation dendrons. To our knowledge, only a single previous example of an  $AB_4$  dendritic building block was available in the literature.<sup>31</sup> Two libraries of hybrid self-

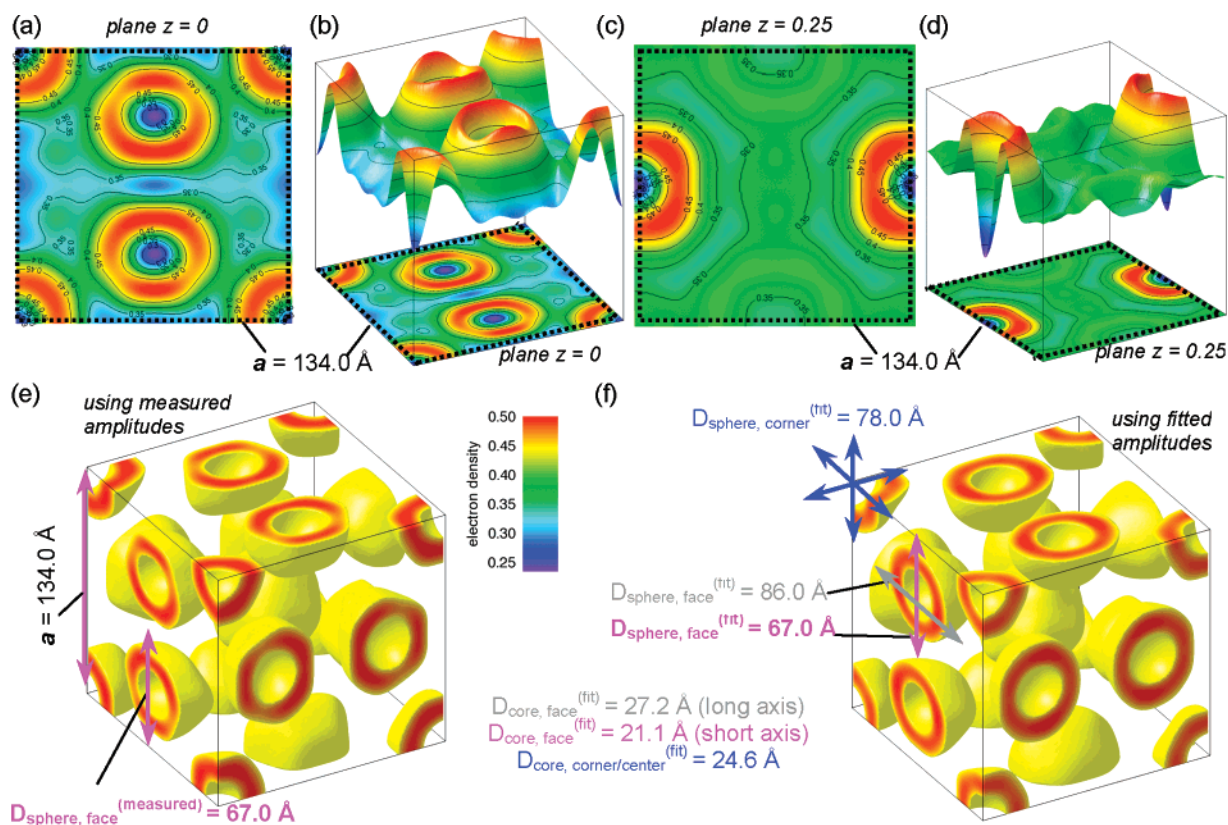


**Figure 8.** Reconstructed electron densities of the  $Pm3n$  lattice generated from (4-AB<sub>4</sub>)12G2-CH<sub>2</sub>OH (40): (a) plane  $z = 0$  in 2-D view and (b) 3-D surface view with vertical axis proportional with the electron density value; (c) plane  $z = 0.25$  in 2-D view and (d) 3-D surface view with vertical axis proportional with the electron density value; (e) unit cell 3-D volumetric electron density; (f) unit cell 3-D volumetric electron density using the fitted amplitudes together with the spheres ( $D_{\text{sphere}}$ ) and less dense center ( $D_{\text{core}}$ ) calculated diameters. In (e,f) only the high electron density regions are shown.

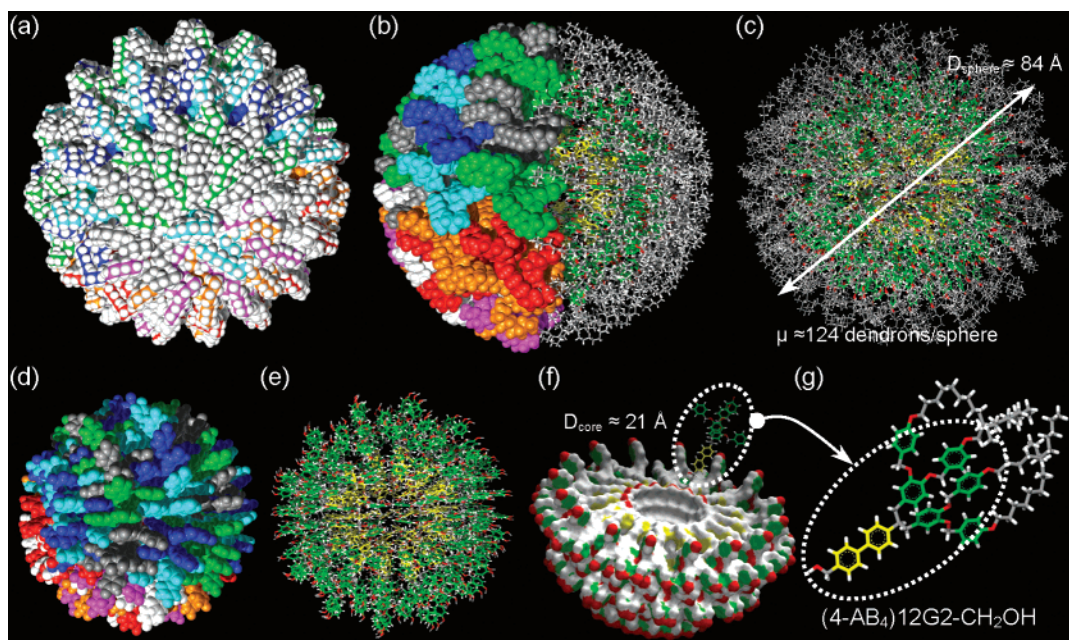


**Figure 9.** Structure of the supramolecular spherical assembly generated from the (4-AB<sub>4</sub>)12G2-CH<sub>2</sub>OH (40): (a) space-filling view, (b) stick and space-filling view with each dendron colored differently, and (c) stick view. The core aromatic region: (d) space-filling view, (e) stick view, and (f) surface view. (g) Dendron structure and color code used in the stick view.

assembling dendrons were synthesized by the functionalization of these new building blocks with benzyl ether dendrons. The structural and retrostructural analysis of the resulting supramolecular dendrimers revealed a high tendency toward the assembly of columnar architectures and allowed the discovery of a

diversity of previously unencountered dendritic conformations: (a) intramolecularly back-folded tapered dendrons with double thickness that self-assemble in pine-tree-like columns with long-range  $7/2$  helical order that extends along more than 46 column strata or more than three full helix turns; (b) tapered

dendrons with the apex tilted or back-folded into the aromatic part of the dendron; (c) crown-like dendrons that self-assemble into long-range 5/1 helical pyramidal columns that extend along at least 40 column strata or 8 helix turns; (d) intramolecularly back-folded conical dendrons that assemble into non-hollow supramolecular spheres; and (e) truncated conical dendrons that self-assemble into spheres with less dense centers. The helical diffraction theory<sup>28</sup> was applied for the first time to the analysis of helical supramolecular dendrimers. The results reported here demonstrated the transfer of complex structural information from the molecular to various supramolecular levels. Last but not least, all other tapered dendrons differ from the tapered dendrons encountered in libraries of self-assembling benzyl ether dendrons

by having their apex back-folded into the aromatic part of the dendron. The generality of these unprecedented dendritic conformations and of their supramolecular structures, as well as the elaboration of new functions based on them, is under investigation and will be reported in future publications.

**Acknowledgment.** Financial support by the National Science Foundation (DMR-0520020 and DMR-0548559) and the P. Roy Vagelos Chair at the University of Pennsylvania is greatly acknowledged. We also thank Prof. Stephen Z. D. Cheng at the University of Akron for density measurements.

**Supporting Information Available:** Experimental procedures with complete spectral, structural, and retrostructural analysis, including Supporting Figures SF1–7 and Supporting Tables ST1–4. This material is available free of charge via the Internet at <http://pubs.acs.org>.

JA073714J

- (31) (a) Bharathi, P.; Zhao, H. D.; Thayumanavan, S. *Org. Lett.* **2001**, *3*, 1961–1964. (b) Jayakumar, K. N.; Bharathi, P.; Thayumanavan, S. *Org. Lett.* **2004**, *6*, 2547–2550. (c) Vutukuri, D. R.; Basu, S.; Thayumanavan, S. *J. Am. Chem. Soc.* **2004**, *126*, 15636–15637. (d) Chen, Y. B.; Ambade, A. V.; Vutukuri, D. R.; Thayumanavan, S. *J. Am. Chem. Soc.* **2006**, *128*, 14760–14761.